

Tris(dibenzo[*a,d*]cycloheptenyl)phosphane: A Bulky Monodentate or Tetrapodal Ligand

Urs Fischbach,^[a] Heinz Rüegger,^[a] and Hansjörg Grützmacher*^[a]

Keywords: Alkene ligands / Gold / Iridium / Palladium / Phosphane ligands / Rhodium / Silver / Tetradentate ligands / Solid-state NMR spectroscopy

The tetradendate phosphane tris(5*H*-dibenzo[*a,d*]cyclohepten-5-yl)phosphane (trop₃P, **1**) was synthesized from tris(trimethylsilyl)phosphane and 5-chloro-5*H*-dibenzo[*a,d*]cycloheptene. Sulfurization of **1** with elemental sulfur led to trop₃P=S. Complexes of **1** with Ag^I, Au^I, Rh^I, Ir^I, and Pd^{II} were prepared. The structures of trop₃P (**1**), trop₃P=S (**2**), [AgCl(trop₃P)] (**3**), [Au(trop₃P)(MeCN)]PF₆ (**5**), [RhCl(trop₃P)] (**6**) and [Pd(trop₃P)(H₂O)](OTf)₂ (**9**) were determined by X-ray diffraction studies. In the coinage metal complexes, **1** serves as monodentate extremely bulky κ¹-phosphane ligand (cone angle ca. 250°). In the Rh^I, Ir^I, and Pd^{II} complexes, **1** acts as

tetradendate ligand. CP MAS NMR spectroscopy shows that the span of the chemical shift tensor increases in **7**, **6**, and **9** in this order (Ω = 310 ppm, 410 ppm, 465 ppm) and contains two strongly deshielded components, which are responsible for the unusual high frequency isotropic shift of the ³¹P resonances. This property correlates inversely with the metal to olefin backbonding ($M \rightarrow C=C_{\text{trop}}$) and $\delta(^{31}\text{P})$ decreases with increasing $M \rightarrow C=C_{\text{trop}}$ in the order **9** (δ = 260 ppm) > **7** (δ = 196 ppm) > **6** (δ = 135 ppm) > **3** (δ = -30.9 ppm). (© Wiley-VCH Verlag GmbH & Co. KGaA, 69451 Weinheim, Germany, 2007)

Introduction

Both phosphanes and alkenes look back on a history of more than one and a half centuries as ligands in metal coordination chemistry.^[1] Metal complexes with these ligands have undergone constant development ever since their discovery. The combination of both types of binding sites in one molecule generates bi- or polydentate ligands and was achieved in the group of Nyholm in the mid-sixties with the synthesis of the first chelating phosphane–alkene ligands.^[2] The most prominent feature of these chelating ligands is their hemilabile character: while the phosphane moiety usually binds quite strongly to a metal center, the olefin is less tightly attached and thus often prone to dissociation. Many different potentially chelating phosphane–olefin ligands have been prepared in the past forty years. Scheme 1 shows selected examples.

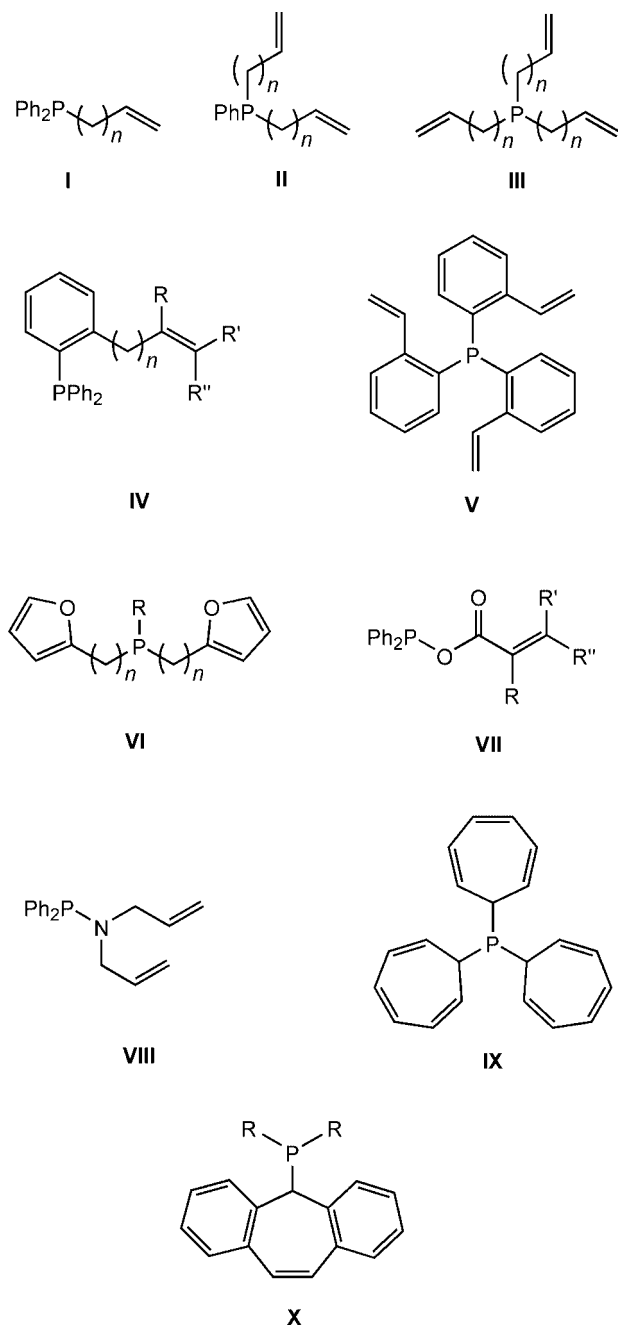
Acyclic alkenylphosphanes are the most obvious type of chelating phosphane–alkene ligands and mono, di- and tri-alkenylphosphanes (**I**, **II** and **III**) have been synthesized and characterized some decades ago.^[3] Their coordination behaviour towards Mo⁰,^[4] W⁰,^[5] Pd^{II},^[6] Pt^{II},^[7] and Rh^I^[8] was investigated. Depending on the size of the resulting chelate ring, alkenylphosphanes act either as monodentate phosphanes or as multidentate chelating ligands, specifically with short chains ($n < 2$) the alkenyl group remains uncoor-

ordinated. Chemical transformations of the alkenyl group (hydrogenation, nucleophilic attack) were observed. Dialkenylphosphanes **II** often bind with one alkenyl group only to the metal center, i.e. they do not serve as tripodal ligands in the electronic ground state structures of the complexes. A large number of *ortho*-alkenylphenylphosphanes (**IV**, **V**) have been prepared^[9] and V⁰,^[10] Cr⁰, Mo⁰,^[11] Mn^I and Re^I,^[12] Fe⁰ and Ru⁰,^[13] Rh^I,^[14] Pd^{II},^[15] and Pt^{II},^[16] Cu^I and Ag^I^[17] complexes were prepared and structurally characterized. Bidentate coordination of the ligands **IV** was established in all complexes. The ligands were prone to addition and isomerization reactions, e.g. hydrogenation or migration of the double bond.

Difurylphosphanes **VI** were applied in the cobalt-catalyzed homologation of methanol and conversions of up to 70% and ethanol selectivities of up to 50% were achieved.^[18] The mixed anhydrides of diphenylphosphinous acid and acrylic acids **VII** may coordinate via the acrylic double bond (observed with Rh^I^[19]) or via the oxygen atom of the carbonyl group (observed with Ru^{II}^[20]). Binding of the double bond in Rh^I complexes is weak and degradation occurred.^[21] A ligand of type **VII** was found to be active in the Rh^I-catalyzed hydrogenation of acrylic acids.^[22] The bidentate phosphane–alkene ligand **VIII** obtained from the condensation of chlorodiphenylphosphane with diallylamine was reported recently. The ligand coordinates to W⁰, Ru^{II}, Rh^I, Pd^{II} and Pt^{II} and both, κ¹:η²- and κ¹-coordination, were observed.^[23]

For Rh^I complexes with type **I**, **III**, **IV** and **V** ligands, trigonal bipyramidal (TBP) structures were observed.^[24]

[a] Department of Chemistry and Applied Biosciences, ETH Zürich, Wolfgang-Pauli-Strasse 10, 8093 Zürich, Switzerland
Fax: +41-44-633-1031
E-mail: gruetzmacher@inorg.chem.ethz.ch



Scheme 1. Mono-, di- and triolefin phosphanes.

This form should be especially favoured by tetradentate tris-(alkenyl)phosphanes like **III** and **V**. While X-ray diffraction studies show that Rh^{I} complexes have the P-donor in the axial and the three C=C donors in the equatorial plane, NMR spectroscopic studies revealed that the latter are fluxional on the NMR time scale and likely dissociate.^[25]

The phosphane cht_3P **IX** (cht = cycloheptatrienyl) was synthesized by Herberhold and co-workers in 1994.^[26] Due to the boat conformation of the seven-membered cht rings, this phosphane is preorganized for binding to a transition metal center by the P-donor and the opposite C=C bonds and stabilization of TBP structures can be expected. However, rotation around the P–C bonds, facile inversion of the

boat conformation of the cht ring, and additional coordination of metals through the C=C bonds adjacent to the P-atom make the ligand fluxional and complicate its coordination chemistry. Indeed a variety of coordination modes are observed in complexes which do not show a special preference for TBP structures, such as V^0 ^[27] (κ^1), Cr^0 , Mo^0 , W^0 ^[28] Mn^{I} ^[29] Fe^0 and Ru^0 ^[30] complexes (κ^1 -, $\kappa^1:\eta^2$ - and $\kappa^1:\eta^4$ -coordination). With Rh^{I} and Ir^{I} the expected trigonal bipyramidal complexes were isolated and these are quite stable, indeed, and it needed other polydentate ligands to displace cht_3P **IX**.^[31] A bidentate coordination mode is observed for **IX** in fluxional Pd^{II} and Pt^{II} dichloride complexes,^[32] but the abstraction of one chloride leads to cationic $[\text{MX}(\text{cht}_3\text{P})]^+$ complexes with TBP structures.^[33] In complexes with Cu^{I} and Ag^{I} , ligand **IX** binds via the P-atom and small but detectable interactions with the opposite C=C bonds of the cht rings were discussed on the basis of solid-state structure data (distances of the metal center to the centroids of the coordinated C=C double bonds in the range of 2.6–3.0 Å were observed^[34,35]).

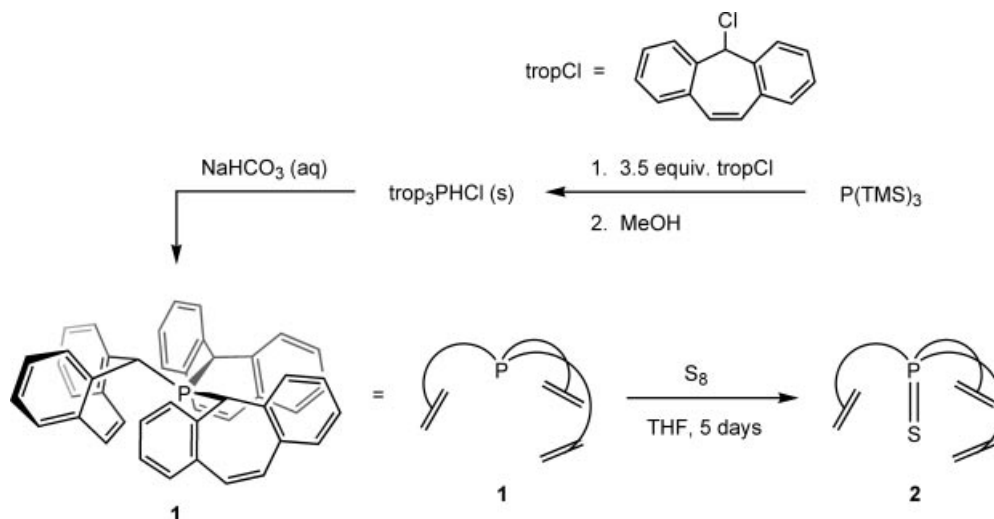
In parallel to the work of Herberhold et al., we started about 10 years ago the investigation of (5*H*-dibenzo[*a,d*]cyclohepten-5-yl)phosphanes **X** as ligands, which we named tropp (from dibenzotroppyliidenylphosphane). The trivial name dibenzotroppyliidenyl (= trop) will be used throughout this paper instead of 5*H*-dibenzo[*a,d*]cyclohepten-5-yl.^[36] The annelated benzo groups make these compounds especially rigid with the phosphanyl substituent in 5-position residing in the energetically preferred *endo*-conformation. A concave binding site results, which is perfectly pre-organized for transition metal binding. A large number of structurally different ligands based on the trop platform^[37] and a variety of complexes with Rh^{I} and Ir^{I} ,^[38] Pd^{II} , Pd^0 , Pt^{II} , Pt^0 ,^[37a–37c,37g] Cu^{I} , Ag^{I} and Au^{I} ^[39] as metal centers were prepared. Noteworthy is the ability of the tropp-type ligands to stabilize complexes with transition metal centers in formally low oxidation states, that is the first stable paramagnetic Rh^0 and Ir^0 complexes could be isolated.^[40]

In the continuation of our work, we report here the synthesis of the ligand tris(5*H*-dibenzo[*a,d*]cyclohepten-5-yl)-phosphane (tropp₃P, **1**) and the synthesis of various transition metal complexes. The coinage metals only exert weak (if any) interactions with the olefinic double bonds, while with Rh^{I} , Ir^{I} and Pd^{II} trigonal bipyramidal complexes are obtained in which the $\text{C}=\text{C}_{\text{trop}}$ groups are tightly bound and tropp₃P acts as tetrapodal ligand.

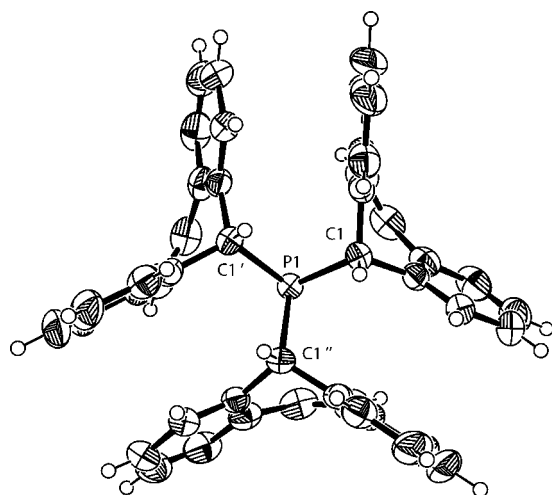
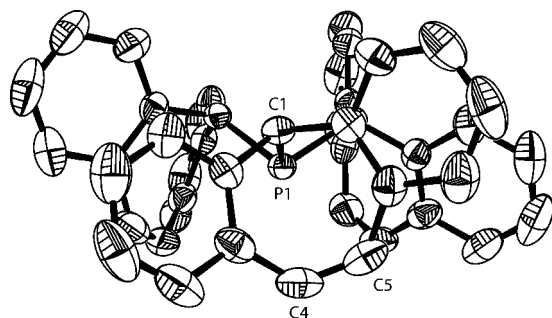
Results and Discussion

Synthesis and Structural Characterization of tropp₃P (**1**)

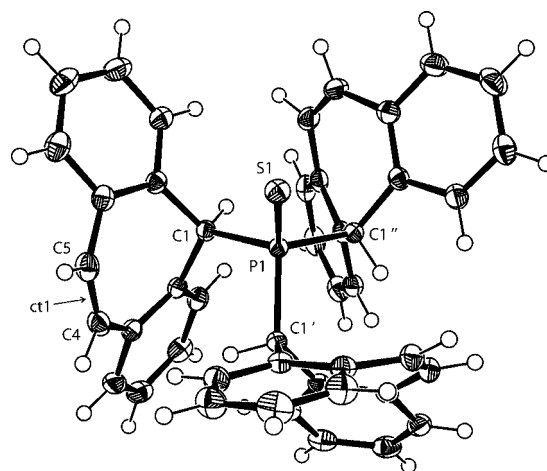
The phosphane tropp₃P was obtained by treating tris(trimethylsilyl)phosphane with 3.5 equiv. of troppCl. The product precipitated from the solution as its hydrochloride salt after the addition of methanol to the reaction mixture and was easily isolated. Further work-up under standard conditions led to the final product (Scheme 2). Tropp₃P can be stored without special precautions on air for at least two

Scheme 2. Synthesis of trop_3P (**1**) and $\text{trop}_3\text{P}=\text{S}$ (**2**).

years and in substance is not oxygenated by 1 atm of O_2 at room temperature. The structure of **1** was determined by X-ray diffraction. Figure 1 and Figure 2 show the molecule

Figure 1. ORTEP plot of trop_3P (**1**) (thermal ellipsoids at 50% probability). View along the threefold symmetry axis of both the molecule and the crystal. Sum of bond angles at P1: 295.5° .Figure 2. ORTEP plot of trop_3P (**1**) (thermal ellipsoids at 50% probability, hydrogen atoms omitted for clarity). View perpendicular to the threefold symmetry axis. Selected bond lengths [Å] and angles [°]: P1–C1: 1.9015(22); C4–C5: 1.330(4); C1–P1–C1': $98.50(9)$. Torsion angles [°]: C1'–P1–C1–C7: $45.14(21)$; C31–P1–C1–C2: $89.98(20)$.

from two different angles; selected bond lengths and angles are given in the Figure caption, pertinent crystal data are given in Table 4. The threefold symmetry axis of the cubic unit cell coincides with the C_3 molecular symmetry axis. There are no mirror planes in the crystal due to the slight twist of the trop moieties and the space group is chiral ($P\bar{4}3n$), that is the crystals exist in two enantiomorphic forms. The prominent structural feature of **1** is the *endo-endo-endo* conformation of the trop_2P substituents at each individual seven-membered ring, which all have a boat conformation. NMR spectra indicate that this highly symmetric structure is also present in solution. Hence, **1** is a highly pre-organized rigid ligand for tetradentate binding in TBP structures with a typical sum of bond angles at the P-atom, $\Sigma^\circ(\text{P}) = 295.5^\circ$.

Figure 3. ORTEP plot of $\text{trop}_3\text{P}=\text{S}$ (**2**) (thermal ellipsoids at 50% probability, solvent molecules omitted for clarity). Selected bond lengths [Å] and angles [°]: P1–S1: 1.9409(9); P1–C1: 1.9181(14); mean C=C (double bond): 1.333(2); S1–P1–C1: $112.42(5)$; C1–P1–C1': $106.37(5)$. Sum of bond angles of the three carbon substituents at P1: 319° . Torsion angle $\varphi(\text{S1–P1–C1–ct1})$: 73.2° .

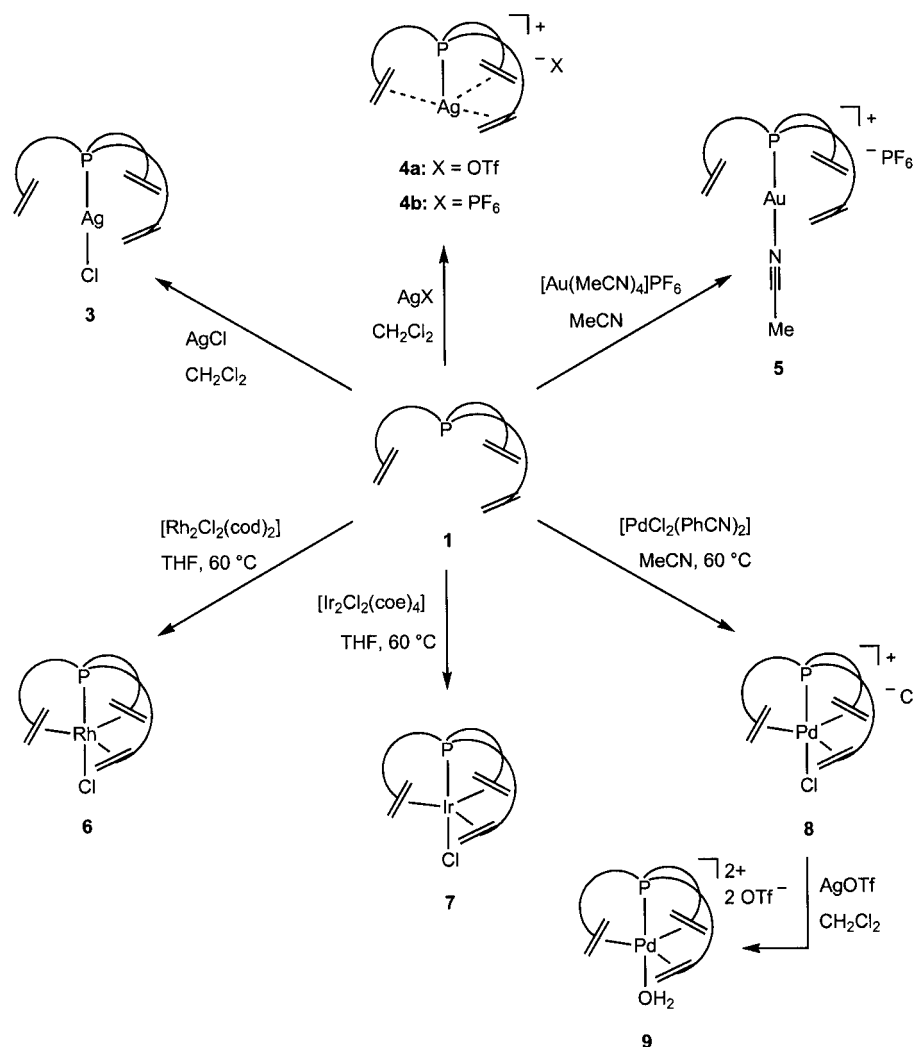
In order to test whether the phosphorus atom can be involved in a chemical reaction, **1** was treated with S_8 (Scheme 2). After stirring in THF at 60 °C for about five days, $\text{trop}_3\text{P}=\text{S}$ (**2**) precipitated and could be isolated (higher reaction temperatures led to decomposition). A plot of the structure obtained by X-ray diffraction is shown in Figure 3 (selected bond lengths and angles are given in the Figure caption, pertinent crystal data are given in Table 4). In contrast to **1**, the trop substituents in **2** are considerably more twisted. This is indicated by the torsion angle $\varphi = \text{X}-\text{P1}-\text{C1}-\text{ct1} = 73.2^\circ$ in **2** vs. $\varphi = 23.0^\circ$ in **1** where X stands for the phosphorus lone pair or a substituent and ct for the centroid of the $\text{C}=\text{C}_{\text{trop}}$ unit (ideally C_{3v} with $\varphi = 0^\circ$, that is the $\text{C}=\text{C}_{\text{trop}}$ group is orthogonal to the P–X vector). As expected, the sum of the C–P–C angles at the phosphorus atom increases to 319° upon sulfurization. Noteworthy is the slight lengthening of the P–C bonds in **2** [1.918(1) Å] with respect to **1** [1.902(2) Å] while usually a shortening is observed upon increasing the formal oxidation state at the phosphorus center to P^{V} .

Metal Complexes of trop_3P

The coordination chemistry of trop_3P (**1**) was investigated through the synthesis of complexes containing the d^{10} noble metal ions, Ag^{I} and Au^{I} , and the d^8 valence electron configured metal ions, Rh^{I} , Ir^{I} and Pd^{II} . The first two metal ions are expected to bind weakly, the latter strongly to the $\text{C}=\text{C}_{\text{trop}}$ units. The coordination to the $\text{C}=\text{C}_{\text{trop}}$ bonds can be evaluated by NMR spectroscopic data and inspection of the molecular structures. Low-frequency ^{13}C NMR resonances for the significantly shielded $\text{C}=\text{C}_{\text{trop}}$ carbon nuclei and torsion angles φ close to 0° are expected when the olefinic units are tightly bound.

Silver and Gold

Despite its low solubility, AgCl is dissolved completely when stirred in a CH_2Cl_2 solution of phosphane **1** at room temperature. After about 20 h $[\text{AgCl}(\text{trop}_3\text{P})]$ (**3**) is quantitatively obtained (Scheme 3). The silver salts AgOTf and



Scheme 3. Synthesis of trop_3P transition metal complexes.

[Ag(MeCN)₄]PF₆ reacted rapidly with **1** to give the complexes [Ag(trop₃P)]OTf (**4a**) and [Ag(trop₃P)]PF₆ (**4b**), respectively. Crystals of the compounds **3**, **4a** and **4b** were grown and investigated by X-ray diffraction. We were unable to refine the data sets of compounds **4a**, **4b** likely because of severe disorder of the OTf[−] and PF₆[−] anions. The structure of **3** was solved and a plot of the structure is shown in Figure 4 (see the Figure caption for selected bond lengths and angles and Table 4 for pertinent crystal data). As expected, P1 and Cl1 coordinate to the Ag center in an almost linear fashion (P1–Ag1–Cl1: 173.1°). The structural data give no indications for coordination of the C=C_{trop} bonds. The mean distance between the Ag atom and the double bond centroids, ct, is approximately 3.2 Å, the C=C_{trop} bonds are not elongated in **3** [C=C_{trop} 1.328(1) Å] with respect to the free phosphane **1** [C=C_{trop} 1.330(4) Å], and the torsion angle φ (Ag1–P1–Cl1–ct1) = 27(7)° remains large.

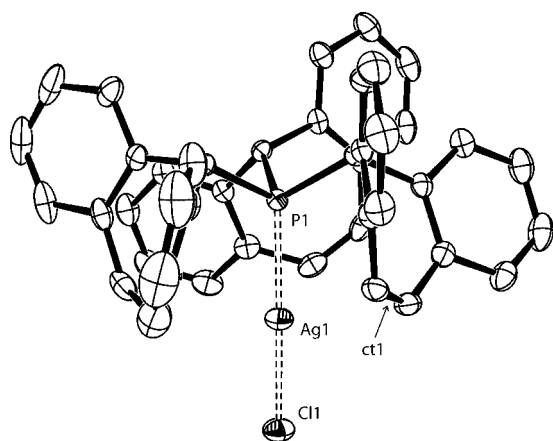


Figure 4. ORTEP plot of [AgCl(trop₃P)] (**3**) (thermal ellipsoids at 30% probability, hydrogen atoms and solvent molecules omitted for clarity, only one of two independent molecules shown). Selected bond lengths [Å] and angles [°]: Ag1–P1: 2.3677(21); Ag1–Cl1: 2.3528(23); mean Ag1–ct: 3.16(12); mean C=C (double bond): 1.328(12); P1–Ag1–Cl1: 173.10(3). Sum of bond angles of the three carbon substituents at P1: 305°. Mean torsion angle φ (Ag1–P1–Cl1–ct1): 27(7)°.

These conclusions are supported by NMR spectroscopy. The element silver consists of two NMR-active isotopes, ¹⁰⁷Ag (51.84%) and ¹⁰⁹Ag (48.16%) with $I = 1/2$. Due to weak coordination and rapid exchange processes, ³¹P NMR spectra of silver phosphane complexes often display a single broad resonance signal at room temperature, which sometimes can be resolved at low temperatures. The silver complex **3** is persistent even at room temperature and the two couplings $^1J(^{107}\text{Ag}, ^{31}\text{P})$ and $^1J(^{109}\text{Ag}, ^{31}\text{P})$ are clearly resolved in the ³¹P NMR spectrum (Figure 5).

A ¹H, ¹⁰⁹Ag HMQC spectrum was measured in order to search for indications of Ag–(CH=CH_{trop}) interactions (Figure 6). The sizeable Ag–H coupling of 9.0 Hz to the benzylic protons (easily observed in the standard ¹H NMR spectrum) gives rise to strong cross peaks in the two-dimensional spectrum. None of the other protons couple strongly enough to generate cross peaks that are detectable above

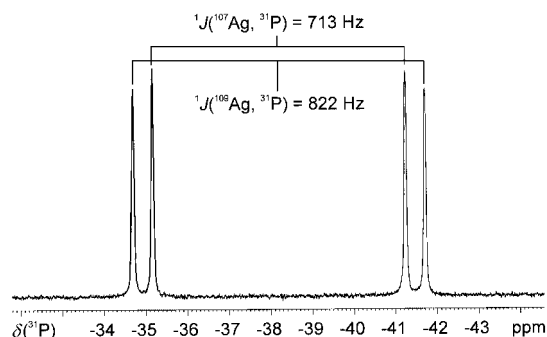


Figure 5. ³¹P NMR spectrum of [Ag(trop₃P)]OTf (**4a**) at room temperature. Coupling to the two almost equally abundant silver isotopes ¹⁰⁷Ag and ¹⁰⁹Ag is clearly resolved.

the noise level. In a second experiment, the Ag–H coupling constants were measured by means of a ³¹P, ¹H HMQC spectrum (Figure 7). Additional nuclei besides ³¹P and ¹H in the spin system will cause a doubling of the resonances in the 2D spectrum. Furthermore, a diagonal displacement of the cross peaks will be observed, which corresponds to the coupling with the additional nuclei. This is clearly visible for the benzylic hydrogen atoms, which do couple with the ¹⁰⁷Ag and ¹⁰⁹Ag nuclei and give eight diagonally displaced cross peaks. Note that from this spectrum individual $^3J(^{109}\text{Ag}, ^1\text{H})$ and $^3J(^{107}\text{Ag}, ^1\text{H})$ coupling constants can be obtained as a consequence of the resolution in the ³¹P domain. Furthermore, the signs of $^3J_{\text{Ag,H}}$ and $^1J_{\text{Ag,P}}$ are the same. For the olefinic protons, only four cross peaks can be

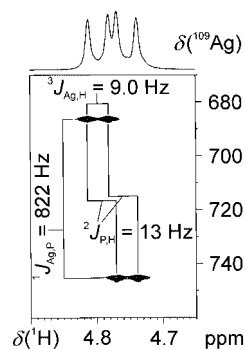


Figure 6. Section of the ¹H, ¹⁰⁹Ag HMQC spectrum of **4a**. Cross peaks with the benzylic protons.

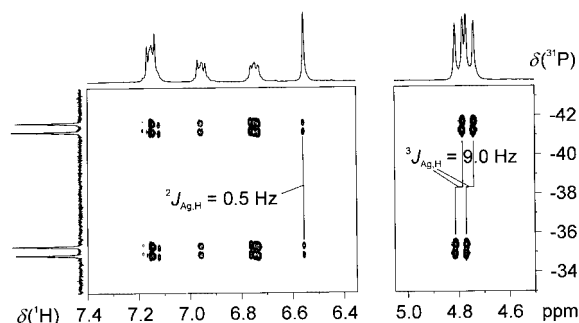


Figure 7. Section of the ¹H, ³¹P HMQC spectrum of **4a**. Ag–H couplings are visible for the benzylic and for the olefinic protons.

recorded, but there is in fact a tiny shift of -0.5 Hz in the ^1H NMR dimension. To the best of our knowledge this is the second coupling constant between a silver nucleus and an olefinic proton that could be measured.^[39] Its small magnitude indicates a very weak and likely dynamic interaction between the $\text{C}=\text{C}_{\text{trop}}$ double bonds and the Ag atom. We note that although the unlike signs of $^2J(\text{Ag}, \text{H}_{\text{olefinic}})$ and $^3J(\text{Ag}, \text{H}_{\text{benzylic}})$ are in agreement with such an explanation, we cannot exclude a coupling mechanism involving just the olefinic proton and extended lone pairs on silver, similar to the ones often encountered in fluorine chemistry. In any case, our data give no indications of metal-to-olefin, $\text{Ag} \rightarrow \text{C}=\text{C}_{\text{trop}}$, π -back-donation and if there were a silver-olefin interaction, this would consist in an olefin to metal, $\text{C}=\text{C}_{\text{trop}} \rightarrow \text{Ag}$, σ -donation within the Dewar–Chatt–Duncanson terminology. This view is fully supported by inspection of the ^{13}C NMR spectroscopic data of the $\text{C}=\text{C}_{\text{trop}}$ carbon nuclei (see Table 2 and the discussion below).

We were especially interested in the synthesis of a monophosphane gold complex, possibly with an additional labile ligand. Therefore we reacted trop_3P (**1**) with $[\text{Au}^{\text{I}}(\text{MeCN})_4]\text{PF}_6$, which was obtained by electrolysis of a gold wire in an acetonitrile solution containing the PF_6^- anion.^[41,42] Upon mixing a suspension of **1** in MeCN with a MeCN solution of $[\text{Au}^{\text{I}}(\text{MeCN})_4]\text{PF}_6$, immediate dissolution of **1** was observed. The product $[\text{Au}(\text{trop}_3\text{P})(\text{MeCN})]\text{PF}_6$ (**5**) was subsequently precipitated by adding toluene (Scheme 3). The structure of **5** is displayed in Figure 8 (see the Figure caption for selected bond lengths and angles and Table 4 for pertinent crystal data obtained by X-ray diffraction). The gold center is coordinated by the phosphorus atom of the trop_3P ligand and a nitrogen atom of the MeCN ligand in a linear coordination sphere ($\text{P1}-\text{Au1}-\text{N1}$ 176.3°). The

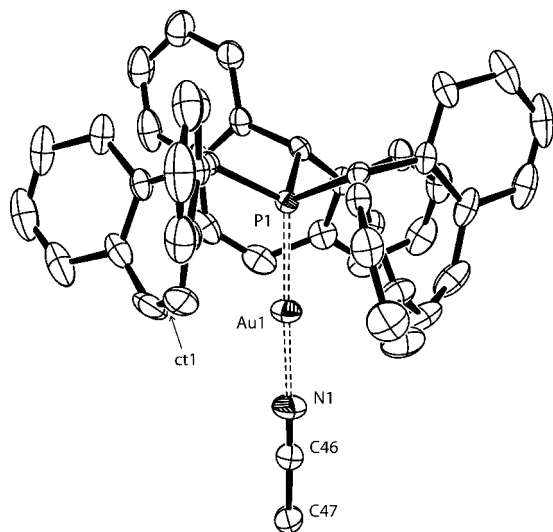


Figure 8. ORTEP plot of $[\text{Au}(\text{trop}_3\text{P})(\text{MeCN})]\text{PF}_6$ (**5**) (thermal ellipsoids at 30% probability, hydrogen atoms and counteranion omitted for clarity). Selected bond lengths [\AA] and angles [$^\circ$]: $\text{Au1}-\text{P1}$: 2.2343(9); $\text{Au1}-\text{N1}$: 2.043(4); mean $\text{Au1}-\text{ct}$: 3.14(6); mean $\text{C}=\text{C}$ (double bond): 1.33(3); $\text{P1}-\text{Au1}-\text{N1}$: $176.30(13)$; $\text{Au1}-\text{N1}-\text{C46}$: $175.5(5)$. Sum of bond angles of the three carbon substituents at P1: 309° . Mean torsion angle $\varphi(\text{Au1}-\text{P1}-\text{C1}-\text{ct1})$: $24(7)^\circ$.

$\text{Au1}-\text{P1}$ and the $\text{Au1}-\text{N1}$ distances are in good accordance with reported bond lengths.^[43] The long distances between the gold atom and surrounding $\text{C}=\text{C}_{\text{trop}}$ groups (average 3.139 \AA) and the twist of the $\text{C}=\text{C}_{\text{trop}}$ units (average $\varphi = 24.4^\circ$) exclude any significant interaction. This is also corroborated by the ^{13}C NMR shifts of the $\text{C}=\text{C}_{\text{trop}}$ units, which again show high frequency shifts upon coordination (see Table 2 below).

Thus, in d^{10} valence electron configured silver and gold complexes, **1** behaves as extremely bulky monodentate phosphane ligand (cone angle approx. 250°)^[44] and the resulting complexes are kinetically inert.

Rhodium, Iridium, and Palladium

When $[\text{Rh}_2(\mu\text{-Cl})_2(\text{cod})_2]$ was treated with **1** in THF at 60°C , quantitative conversion to the desired product $[\text{RhCl}(\text{trop}_3\text{P})]$ (**6**) was observed after 30 h (Scheme 3). Complex **6** precipitated directly from the reaction solution and was isolated as yellow powder by simple filtration. Concentrations higher than 0.03 M should be avoided, because partial decomposition of the ligand with formation of bi(dibenzo[*a,d*]cyclohepten-5-yl), trop_2 , was observed. The structure of **6** was determined by X-ray diffraction. Figure 9 shows a plot, selected bond lengths and angles are listed in the Figure caption, and in Table 4 pertinent crystal data are given. Complex **6** has an almost perfect trigonal bipyramidal structure with the P- and Cl-atoms in the apical and the three $\text{C}=\text{C}_{\text{trop}}$ units in the equatorial positions; the $\text{P1}-\text{Rh1}-\text{Cl1}$ angle is 179° and the $\text{ct}-\text{Rh}-\text{ct}$ angles vary between 119.2° and 121.4° . Clearly, the $\text{C}=\text{C}_{\text{trop}}$ double bonds are coordinated: The averaged $\text{Rh}-\text{ct}$ distances are short (2.15 \AA), the $\text{C}=\text{C}$ bonds are elongated to 1.40 \AA , and the torsion angles φ are smaller than 10° . This leads to an almost perfect parallel stacking of the benzo rings of neighbouring trop groups at distances of about 3.2 \AA . The structural data of **6** very closely match the ones reported for the complex $[\text{RhCl}(\text{cht}_3\text{P})]$ by Herberhold et al.,^[45] only the $\text{Rh}-\text{C}$ distances are marginally shorter by about 1%. Table 1 gives a compilation of selected structure parameters for both compounds.

The iridium complex $[\text{IrCl}(\text{trop}_3\text{P})]$ (**7**) was prepared in about 70% yield when **1** was treated with $[\text{Ir}_2(\mu\text{-Cl})_2(\text{coe})_4]$ for 3 d at 60°C in THF. The reaction is somewhat more sluggish than in the case of the synthesis of **6** but after removal of impurities, **7** is obtained as bright white powder (Scheme 3). Crystals of **7** showed merohedral twinning and we were unable to refine the structure satisfactorily. However, the gross structural features were determined and show that **7** has as expected, a structure analogous to the rhodium complex **6**.

$[\text{PdCl}_2(\text{PhCN})_2]$ reacted with **1** in CH_2Cl_2 at room temperature to form an η^2 complex, likely $[\text{PdCl}_2(\text{trop}_3\text{P})(\text{PhCN})]$ with only one double bond of one trop substituent coordinated, while the phosphorus center and the other two $\text{C}=\text{C}_{\text{trop}}$ bonds remain uncoordinated, which is indicated by the rather low-frequency ^{31}P NMR reso-

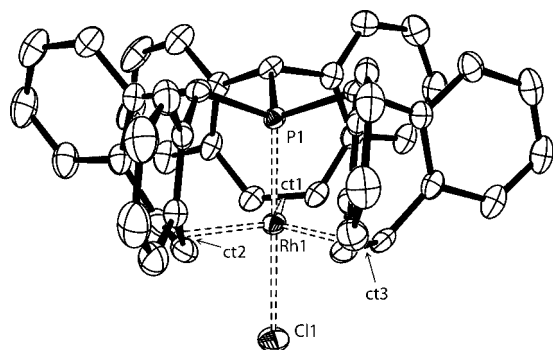


Figure 9. ORTEP plot of $[\text{RhCl}(\text{trop}_3\text{P})]$ (**6**) (thermal ellipsoids at 50% probability, hydrogen atoms and solvent molecules omitted for clarity). Selected bond lengths [Å] and angles [°]: Rh1–P1: 2.1413(8); Rh1–Cl1: 2.4601(8); mean Rh1–ct: 2.150(9); mean C=C (double bond): 1.401(7); P1–Rh1–Cl1: 179.06(3). Sum of bond angles of the three carbon substituents at P1: 320°. Mean torsion angle $\varphi(\text{Rh1–P1–Cl1–ct1})$: 7.1(4)°.

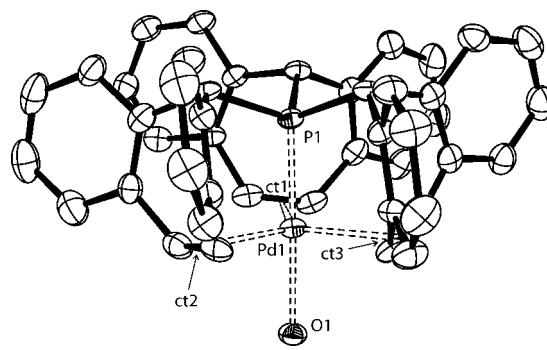


Figure 10. ORTEP plot of $[\text{Pd}(\text{trop}_3\text{P})(\text{H}_2\text{O})](\text{OTf})_2$ (**9**) (thermal ellipsoids at 50% probability, hydrogen atoms, counter anions and solvent molecules omitted for clarity, only one of two independent molecules shown). Selected bond lengths [Å] and angles [°]: Pd1–P1: 2.1736(14); Pd1–O1: 2.142(4); mean Pd1–ct: 2.28(5); mean C=C (double bond): 1.383(20); P1–Pd1–O1: 177.21(11). Sum of bond angles of the three carbon substituents at P1: 322°. Mean torsion angle $\varphi(\text{Pd1–P1–O1–ct1})$: 9.5(8)°.

Table 1. Comparison of structural parameters.

Bond/Angle	$[\text{RhCl}(\text{trop}_3\text{P})]$ (6)	$[\text{RhCl}(\text{cht}_3\text{P})]$ ^[a]
Rh–P	2.1413(8) ^[b] Å	2.153(1) Å
Rh–Cl	2.4601(8) Å	2.460(1) Å
Rh=C	2.265(3) Å	2.283(2) Å
	2.244(3) Å	2.282(2) Å
	2.274(3) Å	2.279(2) Å
	2.248(3) Å	2.280(2) Å
	2.280(3) Å	2.295(2) Å
	2.254(3) Å	2.287(2) Å
P–Rh–Cl	179.06(3)°	178.9(1)°

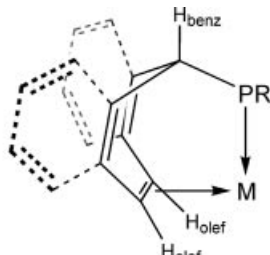
[a] Data from ref.^[45]. [b] Standard deviation.

nance at $\delta = -48.1$ ppm. Performing the reaction in THF or acetonitrile as solvent and heating the reaction mixture to 60 °C for 24 h caused vanishing of the initial yellow color and a red solid started to precipitate. This compound showed a ^{31}P NMR shift at $\delta = 263.8$ ppm and was identified as $[\text{Pd}(\text{trop}_3\text{P})\text{Cl}]\text{Cl}$ (**8**) (Scheme 3). Exchange of the chlorides by triflate anions using AgOTf was a straightforward reaction and gave an intense ruby red solution ($\lambda_{\text{max}} = 497$ nm). From this solution, very dark crystals of the composition $[\text{Pd}(\text{trop}_3\text{P})(\text{H}_2\text{O})](\text{OTf})_2$ (**9**) were obtained which were subjected to a X-ray diffraction study. The dication $[\text{Pd}(\text{trop}_3\text{P})(\text{H}_2\text{O})]^{2+}$ has a TBP structure with the P-atom of the trop_3P ligand and an oxygen atom of a water molecule in the axial positions (Figure 10, see the Figure caption for selected bond lengths and angles and Table 4 for pertinent crystal data). The three $\text{C}=\text{C}_{\text{trop}}$ units are bound in the equatorial positions at about 2.3 Å. This distance is significantly longer (ca. 0.13 Å) than the one in the Rh^{I} complex **6**. The less pronounced $\text{Pd} \rightarrow \text{C}=\text{C}_{\text{trop}}$ π -backbonding also leads to shorter $\text{C}=\text{C}_{\text{trop}}$ bonds (average 1.383 Å) when compared to the Rh^{I} complex **6**. The averaged torsion angle φ is again smaller than 10°. The Pd1–O1 bond length [2.142(4) Å] is very similar to Pd–O distances found in structures of tetracoordinate planar Pd^{II} aqua complexes, while **9** seems to be the first structurally characterized pentacoordinate Pd^{II} aqua complex.

NMR Spectroscopy

Selected ^{31}P , ^1H , and ^{13}C solution NMR spectroscopic data of trop_3P (**1**), $[\text{AgCl}(\text{trop}_3\text{P})]$ (**3**), $[\text{Au}(\text{trop}_3\text{P})(\text{MeCN})]\text{PF}_6$ (**5**), $[\text{RhCl}(\text{trop}_3\text{P})]$ (**6**), $[\text{IrCl}(\text{trop}_3\text{P})]$ (**7**), and $[\text{Pd}(\text{trop}_3\text{P})(\text{H}_2\text{O})](\text{OTf})_2$ (**9**) are listed in entries 1–6 in Table 2.

For comparison we also list the corresponding data for analogous cht_3P complexes (entries 7–12). The proton and ^{13}C NMR spectroscopic data are remarkably similar in both series. The proton in β -position (denoted as H_{benz}) is little influenced by metal coordination to the P-atom as long as the complex remains neutral (especially in the rhodium and iridium complexes, **6** and **7**, respectively). Metal charge has an influence, that is an increasingly positive charge of the complex shifts the H_{benz} resonance to higher frequencies (by 1.63 ppm in the dication **9**, by 0.76 ppm in the mono-cation **5**). Metal to $\text{C}=\text{C}_{\text{trop}}$ π -backbonding, $\text{M} \rightarrow \text{C}=\text{C}_{\text{trop}}$, is reflected in the chemical shifts of the $^{13}\text{C}_{\text{olef}}$ and $^{13}\text{C}_{\text{benz}}$ and to a certain extent in the $^1\text{H}_{\text{olef}}$ nuclei. Increasing π -backbonding causes a low-frequency shift (shielding) of the $^{13}\text{C}_{\text{olef}}$ resonances of the $\text{C}=\text{C}_{\text{trop}}$ units. The data clearly show that $\text{M} \rightarrow \text{C}=\text{C}_{\text{trop}}$ backbonding in the silver and gold complexes is negligible as already stated above, the coordination shifts $\Delta\delta = (\delta_{\text{complex}} - \delta_{\text{free ligand}})$ are even positive (+7 and +5 ppm for **3** and **5**, respectively) while negative $\Delta\delta$ are expected when π -backdonation is significant. This is the case in the Pd^{II} complex **9** ($\Delta\delta = -15.4$), Rh^{I} complex **6** ($\Delta\delta = -45.6$), and Ir^{I} complex **7** ($\Delta\delta = -59.4$) and backbonding increases in this order. The increasing slight shift to lower frequency of the $^{13}\text{C}_{\text{benz}}$ resonance in the same order is a consequence of the increasing bending of the central seven-membered ring upon shortening of the metal $\text{C}=\text{C}_{\text{trop}}$ distances. This effect causes a slight decrease of the sum of the two $\text{P}–\text{C}_{\text{benz}}–\text{C}$ and the $\text{C}–\text{C}_{\text{benz}}–\text{C}$ angle (336.0° in the free phosphane **1**; 334° in **9**, and 331° in **6**). The $^1\text{H}_{\text{olef}}$ resonances are also increasingly shifted to low frequency (by 0.3 ppm in **6**, 0.9 ppm in **7**) upon increasing the metal to olefin backbonding, but this effect is counterbalanced by the formal charge at the metal center and in

Table 2. Comparison of NMR spectroscopic data^[a] for trop₃P and cht₃P complexes.


Compound	Solvent	³¹ P NMR [ppm]	¹ H NMR [ppm] H _{olef}	H _{benz}	¹³ C NMR [ppm] C _{olef}	C _{benz}
trop ₃ P (1)	CDCl ₃	−22.4	6.30	4.16	125.0	55.6
[AgCl(trop ₃ P)] (3)	CD ₂ Cl ₂	−27.7	6.54	4.46	132.0	54.4
[Au(trop ₃ P)(MeCN)]PF ₆ (5)	CD ₃ CN	0.7	6.48	4.92	130.3	54.2
[RhCl(trop ₃ P)] (6)	CD ₂ Cl ₂	191.7	5.93	3.97	79.4	48.4
[IrCl(trop ₃ P)] (7)	CD ₂ Cl ₂	134.1	5.40	4.15	65.6	44.8
[Pd(trop ₃ P)(H ₂ O)](OTf) ₂ (9)	CD ₂ Cl ₂	270.6	7.40	5.79	109.6	51.9
cht ₃ P ^[b]	CDCl ₃	−12.8	6.53	2.32	130.9	36.1
[AgCl(cht ₃ P)] ^[b]	CDCl ₃	−13.8	6.62	2.92	132.0	36.0
[RhCl(cht ₃ P)] ^[c]	CDCl ₃	325.3	5.45	1.94	80.9	35.9
[IrCl(cht ₃ P)] ^[c]	CDCl ₃	265.2	4.81	1.95	65.4	31.1
[PdCl(cht ₃ P)]PF ₆ ^[c]	(CD ₃) ₂ CO	435.9	7.13	3.77	110.6	43.9
[PtCl(cht ₃ P)]PF ₆ ^[c]	(CD ₃) ₂ CO	353.1	6.37	3.60	92.7	36.5

[a] Table includes only chemical shift data; multiplicities and coupling constants are omitted for simplicity. [b] Data from ref.^[35] [c] Data from ref.^[33].

the Pd^{II} complex **9** H_{olef} is even deshielded by 1.1 ppm. The same trends are observed in the cht₃P complexes (see entries 7–12).

A remarkable feature of the M(trop₃P) and M(cht₃P) complexes with M→C=C_{trop} backbonding are the unusual high frequency shifts of the ³¹P resonances. Especially in the Pd^{II} complexes, the ³¹P coordination chemical shifts are almost 300 ppm for **9** and approx. 450 ppm for [Pd(cht₃P)Cl]⁺, which shows likely the least shielded ³¹P nucleus for a seemingly “ordinary” phosphane complex.^[34] Interestingly, this unusual shift to high frequencies becomes smaller when the M→C=C_{trop} backbonding increases, that is in the order Pd > Rh > Ir the ³¹P resonance frequencies decrease. On the contrary, for the d¹⁰-metal complexes, especially for the silver complexes, small coordination shifts of the ³¹P resonance are observed.

In order to gain some insight into these unusual ³¹P NMR shifts, we recorded CP MAS spectra of **1**, **3**, **6**, **7**, and **9**. The top of Figure 11 shows the spectra obtained for **1** and **3** at a spinning frequency of 8 and 7 kHz, respectively. On the bottom of Figure 11, the spectra on static powder samples are displayed. A single sharp resonance with very small side bands is observed for trop₃P (**1**). The spectrum obtained with a non-rotating sample is indicative for an axial chemical shift tensor in complete accordance with the high symmetry determined in the X-ray diffraction study. The anisotropy of the chemical shift tensor, expressed in its span Ω, is about 19 ppm, which is within the expected range for free phosphanes. The ³¹P CP MAS spectrum of [AgCl(trop₃P)] (**3**) at 7 kHz shows a sharp doublet, that is the one bond coupling to silver is resolved under these conditions, but not to the individual ¹⁰⁹Ag and ¹⁰⁷Ag isotopes

(cf. Figure 5). A non-spinning probe showed a typical rhombic signal of moderate band width with Ω ≈ 24 ppm close to the one of the free phosphane **1**.

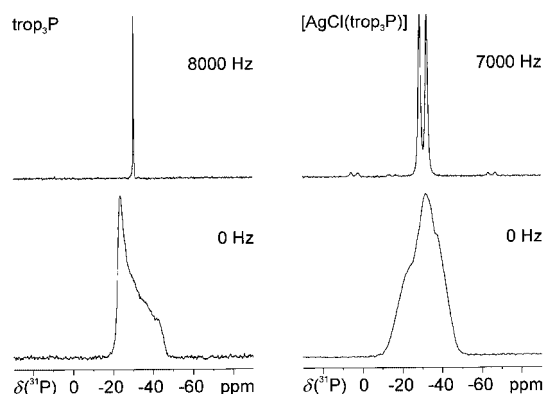


Figure 11. 202 MHz ³¹P{¹H} CP MAS spectra of trop₃P (**1**) and [AgCl(trop₃P)] (**3**) at 8/7 kHz and 0 Hz spinning frequency, respectively.

Figure 12 shows the experimental spectra of [RhCl(trop₃P)] (**6**), [IrCl(trop₃P)] (**7**) and [Pd(trop₃P)(H₂O)]²⁺ (**9**). At 3 kHz rotation frequency of the samples, the spectra observed for **6** and **7** are not significantly different from the axial type (skew κ > 0.9), but a rhombic spectrum is seen for **9** (κ = 0.87). In all cases two components of the chemical shift tensor, δ₁₁ and δ₂₂, were recorded at frequencies typical of weak shielding while the remaining, δ₃₃, was observed at negative values rather similar for all investigated compounds **1–9**. The largest anisotropy Ω ≈ 460 ppm is obtained for the Pd^{II} complex **9**. Clearly, the components δ₁₁ and δ₂₂ are responsible for the isotropic high-frequency shift

Table 3. Compilation of solid state NMR spectroscopic data (ppm) for trop₃P complexes.

Compound	δ_{iso}	δ_{11}	δ_{22}	δ_{33}	$\delta_{\text{iso, calcd.}}$	Ω
trop ₃ P ^[a]	−30.3	−24.0(5)	−24.0(5)	−43.0(5)	−30	19(1)
[AgCl(trop ₃ P)] (3)	−30.9	^[b]	^[b]	^[b]		
[RhCl(trop ₃ P)] (6) ^[c]	196	330(5)	330(5)	−70(5)	197	400(10)
[IrCl(trop ₃ P)] (7) ^[c]	135	245(5)	245(5)	−85(5)	135	330(10)
[Pd(trop ₃ P)(H ₂ O)](OTf) ₂ (9) ^[c]	260	425(5)	395(5)	−40(5)	260	465(10)

[a] Values determined by line shape analysis at 0 Hz spinning frequency. [b] The contributions of the anisotropies of scalar coupling, dipolar coupling and chemical shift can not be separated satisfactorily. [c] Values determined by analysis of the experimental MAS spectrum and then fitting a simulation.

recorded in solution. Simulation of the spectra led to the chemical shift tensor elements listed in Table 3. The axial spectra of **6** and **7** allow to conclude that the δ_{33} element is aligned with the M–P vector and δ_{11} and δ_{22} are consequently orthogonal to M–P and parallel to the equatorial coordination plane with the metal C=C_{trop} arrangement.^[46] As Table 3 shows, the deshielding of δ_{11} and δ_{22} decreases in the order **9** < **6** < **7** as the M→C=C_{trop} backbonding increases.

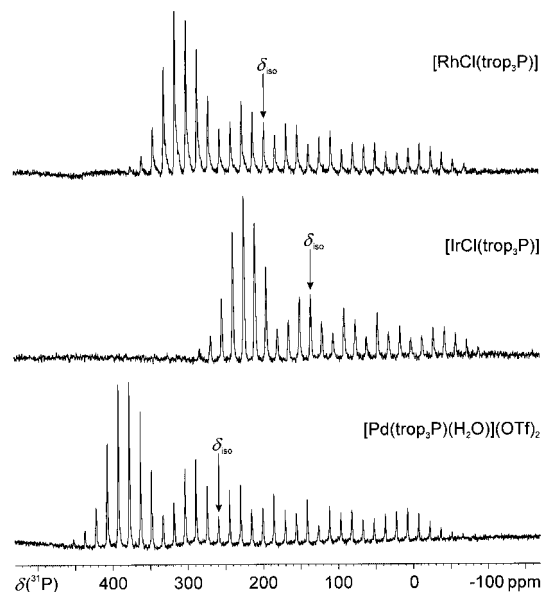


Figure 12. 202 MHz ³¹P{¹H} CP MAS spectra of [RhCl(trop₃P)] (6) (top), [IrCl(trop₃P)] (7) (middle) and [Pd(trop₃P)(H₂O)](OTf)₂ (9) (bottom) at 3 kHz rotation frequency.

Conclusions

The new phosphane trop₃P was synthesized in an unexpected simple manner from P(SiMe₃)₃ and 5-chlorodibenzo[*a,d*]cycloheptene, tropCl. The structure of trop₃P is very rigid and the phosphorus atom is deeply embedded in a concave pocket formed by the three trop substituents. This makes the phosphane infinitely stable against oxidation on air and long reaction times are needed for converting trop₃P into the corresponding thiophosphorane, trop₃P=S, or to bind transition metals into the pocket. In complexes with d¹⁰ valence electron configured metal complexes, trop₃P be-

haves as an extremely bulky monodenate ligand with a cone angle of approx. 250°. Consequently, complexes of Ag^I and Au^I are kinetically stabilized and the isolation of a rare stable cationic monophosphane acetonitrile complex [Au(trop₃P)(MeCN)]⁺ (**5**) was achieved.^[47] Although questionable a silver–olefin interaction exists in compounds like [Ag(C₂H₄)₃]⁺ Al[OC(CF₃)₃]₄[−],^[48] our data do not support the idea that any significant interaction (in the sense of a chemical bond formed by orbital overlap) exists in linearly coordinated ML₂ complexes where M = Ag⁺ or Au⁺, which have additional olefinic moieties in close proximity. In complexes with d⁸ valence electron configured transition metals, trop₃P serves as tetradentate ligand and trigonal pyramidal [M(trop₃P)] fragments were observed^[49] with M = Rh^I, Ir^I, and Pd^{II} to which a fifth ligand X = Cl[−], H₂O binds in the remaining axial position. Structural and NMR spectroscopic data suggest that π-backbonding from filled d-orbitals at the transition metal center to the π* orbitals of the coordinated C=C double bonds increases as expected in the order Pd^{II} < Rh^I < Ir^I. Remarkably, the ³¹P NMR shifts react most sensitively to this effect and a decrease in M→C=C_{trop} backbonding causes a strong deshielding, that is shifts to higher frequencies. ³¹P CP MAS NMR spectroscopy allowed the chemical shift tensor to be determined and shows that the unusual deshielding of the ³¹P nuclei in the [MX(trop₃P)] complexes is caused by large positive δ_{11} and δ_{22} components, which are in plane with the three coordinated C=C_{trop} units and the metal center M = Pd^{II}, Rh^I, Ir^I. The third component, δ_{33} , is aligned with the M–P bond and has similar negative values for all complexes. Under the assumption that the ³¹P NMR shift is dominated by the paramagnetic shift term, excitations into unoccupied orbitals are likely responsible for this phenomenon. We suggest that these relevant unoccupied orbitals are those which correspond to an antibonding interaction between a filled d-orbital at the metal center and the π*-orbital of the C=C_{trop} bond. A strong M→C=C_{trop} backbonding will stabilize the bonding d(M)–π*(C=C) interaction at low energies but lift the antibonding d(M)–π*(C=C) interaction to high energies. Inversely, a weak M→C=C_{trop} backbonding will create an energetically low lying antibonding d(M)–π*(C=C) interaction and excitations into this orbital are made responsible for the exceptional coordination shifts leading to unusually high-frequency-shifted ³¹P resonances in the Pd^{II} complexes { $\delta(^{31}\text{P})$ = 270.6 ppm in [Pd(trop₃P)(H₂O)]²⁺}; [$\delta(^{31}\text{P})$ = 435.9 ppm in [Pd(cht₃P)(Cl)]⁺]. For

a detailed explanation of this phenomenon, an in-depth quantum chemical analysis is needed, which however was beyond the scope of this study.

Experimental Section

General Procedures: All manipulations of air- or moisture-sensitive compounds were performed on a standard vacuum line in flame-dried flasks under an atmosphere of argon. Solvents were distilled under argon from Na (toluene), Na/benzophenone (THF, diethyl ether), Na/benzophenone/tetraglyme (*n*-hexane), CaH₂ (CH₂Cl₂, chloroform, acetonitrile), P₂O₅ (acetonitrile). Air-sensitive compounds were stored and weighed in gloveboxes. Basic chemicals were ordered from commercial suppliers and used as received. The following organic compounds and metal precursors were prepared according to literature methods: tropCl,^[50] (TMS)₃P,^[51] [Ir₂(COE)₄(μ-Cl)₂].^[52] IR spectra were recorded on a Perkin–Elmer Spectrum 2000 FT-IR-Raman spectrometer with the ATR technique. Mass spectra of organic compounds were recorded on a Finnigan MAT SSQ 7000 mass spectrometer using electron ionization. Melting points were determined with a Büchi melting point apparatus and are not corrected. UV/Vis spectra were recorded on a UV/Vis/NIR lambda 19 spectrometer in 5-mm quartz cuvettes (200–1000 nm). Solution NMR spectra were recorded on Bruker Avance 400, 300, 250 and 200 spectrometers. Chemical shifts (δ) are measured and referenced according to IUPAC^[53] and expressed in ppm. ³¹P CP MAS solid state NMR spectra were acquired at room temperature on a Bruker Avance instrument operating at a ¹H Larmor frequency of 500 MHz. Conventional cross-polarization and magic-angle-spinning techniques were implemented by using 4-mm rotors with which rotational frequencies of at least 11 kHz were achieved. The strength of the magnetic field was adjusted such that the ¹³C carboxylate resonance of α -glycine appeared at δ = 176.0 ppm. In consequence referencing of all isotopes could be achieved as for the solution NMR using the unified \mathcal{E} scale.^[53] Chemical shifts are expressed relative to H₃PO₄. CP MAS spectra were simulated by using the SIMPSON program package.^[54]

Preparation of Tris(5*H*-dibenzo[*a,d*]cyclohepten-5-yl)phosphane (1): TropCl (13.4 g, 59 mmol) was placed under argon in a 500-mL round-bottom Schlenk flask. It was dissolved in 250 mL freshly distilled, dry THF. P(SiMe₃)₃ (4.5 mL, 3.9 g, 16 mmol) was added dropwise to this solution. The resulting mixture was stirred at room temperature for several days and the reaction was monitored by ³¹P NMR spectroscopy. The first substitution leading to trop(SiMe₃)₂P [δ (³¹P) = −148.2 ppm] is quite fast, the second step to trop₂-(SiMe₃)P [δ (³¹P) = −70.3 ppm] and third step to **1** proceed more slowly. When the ³¹P NMR spectrum showed almost complete conversion to trop₃P **1** (after 4 to 6 d), MeOH (2.5 mL, 2.0 g, 62 mmol) was added and stirring was continued for another 12 h. During this time a white precipitate formed in the reaction mixture (trop₃P·HCl) [δ (³¹P) = −45.5 (¹J_{P,H} = 480 Hz) ppm]. This precipitate was collected by filtration and washed with THF. The product was obtained by suspending (trop₃P·HCl) in a concentrated NaHCO₃ solution and extracting the resulting mixture twice with CH₂Cl₂. The combined organic phases were dried with Na₂SO₄ and concentrated to dryness. The product was dried in high vacuum giving a fine white powder of high purity. If necessary, **1** can be further purified by recrystallization from toluene. Yield: 7.54 g (80%). M.p. 247 °C. C₄₅H₃₃P (604.72): calcd. C 89.38, H 5.50, P 5.12; found C 89.12, H 5.66. IR (ATR): $\tilde{\nu}$ = 3013 (w, ν_{CH}), 1592 (w), 1488 (m), 1453 (m), 1432 (m), 1329 (m), 1287 (m), 796 (s), 781 (s), 728 (s),

633 (s) cm^{−1}. MS (EI): *m/z* 603 (M⁺), 191 (C₁₅H₁₁⁺). ¹H NMR (300 MHz, CDCl₃, 25 °C): δ = 4.16 (d, ²J_{P,H} = 1.8 Hz, 3 H, H_{benz}), 6.30 (s, 6 H, H_{olef}), 6.44–6.51 (m, 6 H, H_{aryl}), 6.81–6.87 (m, 6 H, H_{aryl}), 6.97–7.06 (m, 12 H, H_{aryl}) ppm. ¹³C{¹H} NMR (75.5 MHz, CDCl₃, 25 °C): δ = 55.6 (d, ¹J_{P,C} = 36.3 Hz, 3 C, C_{benz}), 125.0 (d, ¹J_{P,C} = 0.7 Hz, 6 C, C_{olef}), 128.3 (s, 6 C, C_{aryl}), 128.6 (s, 6 C, C_{aryl}), 128.6 (d, ¹J_{P,C} = 3.1 Hz, 6 C, C_{aryl}), 131.6 (d, ¹J_{P,C} = 5.7 Hz, 6 C, C_{aryl}), 135.4 (d, ¹J_{P,C} = 3.5 Hz, 6 C, C_{aryl}), 139.3 (d, ¹J_{P,C} = 9.0 Hz, 6 C, C_{aryl}) ppm. ³¹P{¹H} NMR (121.5 MHz, CDCl₃, 25 °C): δ = −22.7 (s) ppm.

Preparation of Tris(5*H*-dibenzo[*a,d*]cyclohepten-5-yl)phosphane Sulfide (2): In a Schlenk flask, trop₃P (240 mg, 0.40 mmol) and S₈ (14 mg, 0.44 mmol) were suspended in THF (20 mL). This mixture was heated to 60 °C and stirred for several days. Conversion was about 20% after 17 h and about 40% after 40 h. After five days, a white precipitate had formed, which was collected by filtration and washed with THF. The filtrate still contained about 50% starting material. The collected product was dried in high vacuum to give a microcrystalline white solid. Yield: 35 mg (14%). M.p. 212 °C. C₄₅H₃₃PS (636.78): calcd. C 84.88, H 5.22, P 4.86; found C 84.43, H 4.91. IR (ATR): $\tilde{\nu}$ = 3017 (w, ν_{CH}), 2972 (w, ν_{CH}), 2852 (w, ν_{CH}), 1494 (m), 1456 (m), 1432 (m), 1160 (m), 1065 (m), 803 (s), 779 (s), 769 (s), 726 (s), 687 (s), 615 (m). ¹H NMR (300 MHz, CD₂Cl₂, 25 °C): δ = 5.39 (d, ²J_{P,H} = 16 Hz, 3 H, H_{benz}), 6.34 (br. s, 6 H, H_{olef}), 7.10–7.25 (m, 12 H, H_{aryl}), 7.25–7.40 (m, 6 H, H_{aryl}), 7.40–7.50 (m, 12 H, H_{aryl}) ppm. ¹³C{¹H} NMR (75.5 MHz, CD₂Cl₂, 25 °C): δ = 59.5 (d, ¹J_{P,C} = 23.5 Hz, 3 C, C_{benz}), 127.3 (s, 6 C, C_{olef}), 128.8 (s, 6 C, C_{aryl}), 129.9 (s, 6 C, C_{aryl}), 131.7 (d, ¹J_{P,C} = 6.5 Hz, 6 C, C_{aryl}), 133.2 (s, 6 C, C_{aryl}), 135.8 (s, 6 C, C_{aryl,quat}), 136.0 (s, 6 C, C_{aryl,quat}) ppm. ³¹P{¹H} NMR (121.5 MHz, CD₂Cl₂, 25 °C): δ = 79.5 (s) ppm.

Preparation of Chloro[tris(5*H*-dibenzo[*a,d*]cyclohepten-5-yl)phosphane]silver(I) (3): Aqueous solutions of AgNO₃ (2.0 g, 12 mmol) and NH₄Cl (1.0 g, 19 mmol) were aggregated to precipitate AgCl. This precipitate was collected by filtration, washed with water, ethanol and diethyl ether and dried on air. trop₃P **1** (158 mg, 0.26 mmol) and an excess of the freshly precipitated AgCl (123 mg, 0.86 mmol) were combined in CH₂Cl₂ (20 mL). This mixture was stirred for 16 h. The remaining AgCl was removed by filtration and washed with CH₂Cl₂. The filtrate was concentrated to dryness. Then the product was washed with small amounts of pentane and dried in high vacuum. The product was obtained as a bright white microcrystalline solid. Yield: 135 mg (69%). M.p. 251–260 °C (decomposition). C₄₅H₃₃AgClP (748.04): calcd. C 72.25, H 4.45, P 4.14; found C 71.98, H 4.58. IR (ATR): $\tilde{\nu}$ = 3017 (w, ν_{CH}), 1594 (w), 1486 (m), 1455 (m), 1434 (m), 1334 (m), 1296 (m), 798 (s), 785 (s), 729 (s), 637 (s) cm^{−1}. ¹H NMR (300 MHz, CD₂Cl₂, 25 °C): δ = 4.46 (dd, ²J_{P,H} = 12 Hz, ³J_{Ag,H} = 7.8 Hz, 3 H, H_{benz}), 6.54 (s, 6 H, H_{olef}), 6.56 (d br, ³J_{H,H} = 7.2 Hz, 6 H, H_{aryl}), 7.01 (dd, ³J_{H,H} = 7.2 Hz, ⁴J_{H,H} = 1.8 Hz, 6 H, H_{aryl}), 7.16 (ddd, ³J_{H,H} = 7.2 Hz, 7.2 Hz; ⁴J_{H,H} = 1.8 Hz, 6 H, H_{aryl}), 7.20 (dd br, ³J_{H,H} = 7.2 Hz, 7.2 Hz; 6 H, H_{aryl}) ppm. ¹³C{¹H} NMR (75.5 MHz, CD₂Cl₂, 25 °C): δ = 54.4 (dd, ¹J_{P,C} = 5.7 Hz, ²J_{Ag,C} = 1.5 Hz, 3 C, C_{benz}), 126.7 (d, ¹J_{P,C} = 1.7 Hz, 6 C, C_{aryl}), 129.2 (s, 6 C, C_{aryl}), 129.4 (d, ³J_{P,C} = 4.6 Hz, 6 C, C_{aryl}), 129.5 (d, ¹J_{P,C} = 1.7 Hz, 6 C, C_{aryl}), 132.0 (dd, ⁴J_{P,C} = 5.3 Hz, ¹J_{Ag,C} = 2.0 Hz, 6 C, C_{olef}), 135.0 (d, ¹J_{P,C} = 4.6 Hz, 6 C, C_{aryl,quat}), 136.0 (d, ¹J_{P,C} = 3.3 Hz, 6 C, C_{aryl,quat}) ppm. ³¹P{¹H} NMR (121.5 MHz, CD₂Cl₂, 25 °C): δ = −27.7 (d, ¹J_{107Ag,P} = 669 Hz, ¹J_{109Ag,P} = 771 Hz) ppm.

Preparation of [Tris(5*H*-dibenzo[*a,d*]cyclohepten-5-yl)phosphane]silver(I) Trifluoromethanesulfonate (4a): In a Schlenk flask, trop₃P **1** (480 mg, 0.79 mmol) was dissolved in THF. AgOTf (204 mg,

0.79 mmol) was added to this solution and the resulting mixture was stirred for three days. Any precipitates were removed by filtration through celite. The filtrate was concentrated to about one third of its volume and left at -20°C for crystallization. The precipitated product was collected by filtration and dried in high vacuum. The product was an off-white powder. Yield: 360 mg (53%). M.p. $223\text{--}228^{\circ}\text{C}$ (decomposition). Due to the light sensitivity of the compound, we were not able to obtain reliable elemental analytical data. IR (ATR): $\tilde{\nu} = 3362(\text{br.}, \nu_{\text{H}_2\text{O}})$, $3020(\text{w}, \nu_{\text{CH}})$, $1594(\text{w})$, $1489(\text{m})$, $1455(\text{m})$, $1434(\text{m})$, $1330(\text{m})$, $1265(\text{s})$, $1234(\text{s})$, $1156(\text{s})$, $1027(\text{s})$, $802(\text{s})$, $788(\text{s})$, $763(\text{s})$, $732(\text{s})$, $635(\text{s})\text{ cm}^{-1}$. ^1H NMR (300 MHz, CD_3CN , 25°C): $\delta = 4.78(\text{dd}, ^2J_{\text{P,H}} = 13\text{ Hz}, ^3J_{\text{Ag,H}} = 9.0\text{ Hz}, 3\text{ H}, \text{H}_{\text{benz}})$, $6.56(\text{s}, 6\text{ H}, \text{H}_{\text{olef}})$, $6.71\text{--}6.78(\text{m}, 6\text{ H}, \text{H}_{\text{aryl}})$, $6.92\text{--}6.99(\text{m}, 6\text{ H}, \text{H}_{\text{aryl}})$, $7.10\text{--}7.19(\text{m}, 12\text{ H}, \text{H}_{\text{aryl}})$ ppm. $^{13}\text{C}\{^1\text{H}\}$ NMR (75.5 MHz, CD_3CN , 25°C): $\delta = 52.9(\text{dd}, ^1J_{\text{P,C}} = 5.6\text{ Hz}, ^2J_{\text{Ag,C}} = 3.6\text{ Hz}, 3\text{ C}, \text{C}_{\text{benz}})$, $126.6(\text{d}, ^5J_{\text{P,C}} = 1.5\text{ Hz}, 6\text{ C}, \text{C}_{\text{g}})$, $129.2(\text{d}, ^4J_{\text{P,C}} = 1.7\text{ Hz}, 6\text{ C}, \text{C}_{\text{h}})$, $129.6(\text{d}, ^3J_{\text{P,C}} = 4.6\text{ Hz}, 6\text{ C}, \text{C}_{\text{e}})$, $129.9(\text{s}, 6\text{ C}, \text{C}_{\text{f}})$, $131.2(\text{dd}, ^4J_{\text{P,C}} = 6.0\text{ Hz}, ^1J_{\text{Ag,C}} = 1.7\text{ Hz}, 6\text{ C}, \text{C}_{\text{olef}})$, $134.1(\text{d}, ^3J_{\text{P,C}} = 4.5\text{ Hz}, 6\text{ C}, \text{C}_{\text{e}})$, $135.6(\text{d}, ^2J_{\text{P,C}} = 2.7\text{ Hz}, 6\text{ C}, \text{C}_{\text{b}})$ ppm. $^{19}\text{F}\{^1\text{H}\}$ NMR (188.3 MHz, CD_3CN , 25°C): $\delta = -79.2(\text{s})$ ppm. $^{31}\text{P}\{^1\text{H}\}$ NMR (121.5 MHz, CD_3CN , 25°C): $\delta = -38.3(\text{d}, ^1J_{107\text{Ag,P}} = 713\text{ Hz}, ^1J_{109\text{Ag,P}} = 822\text{ Hz})$ ppm. $^{109}\text{Ag}\{^1\text{H}\}$ NMR (13.4 MHz, CD_3CN , 25°C): $\delta = 717(\text{d}, ^1J_{\text{Ag,P}} = 822\text{ Hz})$ ppm.

Preparation of [Tris(5*H*-dibenzo[*a,d*]cyclohepten-5-yl)phosphane]silver(I) Hexafluorophosphate (4b): A solution of trop₃P **1** (195 mg, 0.33 mmol) in THF was added dropwise to a solution of [Ag(MeCN)₂]₂PF₆ (110 mg, 0.33 mmol) in THF. The reaction mixture was left overnight under strict exclusion of light for crystallization. The precipitated product was collected by filtration and dissolved in acetonitrile. Impurities were removed by filtration and the filtrate was concentrated to dryness. Recrystallization from THF and drying in high vacuum yielded the product as a slightly off-white microcrystalline powder. Yield: 131 mg (47%). M.p. $198\text{--}202^{\circ}\text{C}$ (decomposition). Due to the light sensitivity of the compound, we were not able to obtain reliable elemental analytical data. IR (ATR): $\tilde{\nu} = 3057(\text{w}, \nu_{\text{CH}})$, $1595(\text{w})$, $1490(\text{w})$, $1455(\text{w})$, $1434(\text{w})$, $1330(\text{w})$, $1295(\text{w})$, $834(\text{s})$, $803(\text{s})$, $788(\text{m})$, $765(\text{m})$, $734(\text{m})$, $637(\text{m})\text{ cm}^{-1}$. ^1H NMR (300.1 MHz, CD_3CN , 25°C): $\delta = 4.76(\text{dd}, ^2J_{\text{P,H}} = 12.9\text{ Hz}, ^3J_{\text{Ag,H}} = 9.0\text{ Hz}, 3\text{ H}, \text{H}_{\text{benz}})$, $6.55(\text{s}, 6\text{ H}, \text{H}_{\text{olef}})$, $6.71\text{--}6.78(\text{m}, 6\text{ H}, \text{H}_{\text{aryl}})$, $6.92\text{--}6.99(\text{m}, 6\text{ H}, \text{H}_{\text{aryl}})$, $7.12\text{--}7.21(\text{m}, 12\text{ H}, \text{H}_{\text{aryl}})$ ppm. $^{19}\text{F}\{^1\text{H}\}$ NMR (188.3 MHz, CD_3CN , 25°C): $\delta = -72.8(\text{d}, ^1J_{\text{P,F}} = 706\text{ Hz})$ ppm. $^{31}\text{P}\{^1\text{H}\}$ NMR (121.5 MHz, CD_3CN , 25°C): $\delta = -37.9(\text{d}, ^1J_{107\text{Ag,P}} = 715\text{ Hz}, ^1J_{109\text{Ag,P}} = 825\text{ Hz}, \text{trop}_3\text{P})$, $-144.5(\text{hept}, ^1J_{\text{P,F}} = 706\text{ Hz}, \text{PF}_6)$ ppm.

Preparation of (Acetonitrile)[tris(5*H*-dibenzo[*a,d*]cyclohepten-5-yl)phosphane]gold(I) Hexafluorophosphate (5): Due to the strong oxidizing potential of Au^I this synthesis was carried out under inert conditions. The precursor complex [Au(MeCN)₄]₂PF₆ was synthesized using a slightly modified published procedure.^[41] [Au(MeCN)₄]⁺ is generated by oxidation of a gold wire in an electrolysis apparatus. The anode consisted of a coiled gold wire, whereas for the cathode a coiled silver wire was used. The three compartments were separated by two anion-selective membranes. [Ag(MeCN)₂]₂PF₆ (1.67 g, 4.99 mmol) and Me₄NPF₆ (1.29 g, 5.9 mmol) were dissolved in acetonitrile (50 mL) and transferred into the cathodic compartment. The bridge compartment was filled with Me₄NPF₆ (1.33 g, 6.1 mmol) dissolved in acetonitrile (30 mL). To neat acetonitrile (50 mL) in the anodic compartment, 0.5 mL of a solution of Et₄NI ($6\cdot 10^{-4}\text{ M}$, $3\cdot 10^{-4}\text{ mmol}$) were added (the resulting solution was $6\cdot 10^{-6}\text{ M}$ in Et₄NI). The iodide catalytically activated the surface of the gold wire. After the electrolysis the product solution in the anodic compartment was separated by cannula

filtration from colloidal Au⁰ precipitates and used immediately afterwards. Separately, trop₃P **1** (0.19 g, 0.31 mmol) was suspended in freshly distilled acetonitrile (50 mL). Then the decanted solution of [Au(MeCN)₄]₂PF₆ in acetonitrile was added dropwise until the reaction mixture became clear (about 15 mL). Toluene was added until some precipitate started to form. Leaving the mixture at room temperature overnight gave cubic shaped crystals suitable for X-ray diffraction (50 mg, 16%). Further product was obtained by concentration of the solution and was collected by filtration. The slightly yellow micro-crystalline powder was washed with toluene and dried in high vacuum. Yield: 236 mg (76%). M.p. $208\text{--}212^{\circ}\text{C}$ (decomposition). IR (ATR): $\tilde{\nu} = 3021(\text{w}, \nu_{\text{CH}})$, $1491(\text{m})$, $1455(\text{m})$, $1433(\text{m})$, $1334(\text{m})$, $1301(\text{m})$, $834(\text{s})$, $797(\text{s})$, $763(\text{s})$, $734(\text{s})$, $641(\text{m})\text{ cm}^{-1}$. ^1H NMR (300 MHz, CD_3CN , 25°C): $\delta = 4.92(\text{d}, ^2J_{\text{P,H}} = 15\text{ Hz}, 3\text{ H}, \text{H}_{\text{benz}})$, $6.48(\text{s}, 6\text{ H}, \text{H}_{\text{olef}})$, $6.67\text{--}6.73(\text{m}, 6\text{ H}, \text{H}_{\text{aryl}})$, $7.02\text{--}7.07(\text{m}, 6\text{ H}, \text{H}_{\text{aryl}})$, $7.18\text{--}7.30(\text{m}, 12\text{ H}, \text{H}_{\text{aryl}})$ ppm. $^{13}\text{C}\{^1\text{H}\}$ NMR (75.5 MHz, CD_3CN , 25°C): $\delta = 54.2(\text{d}, ^1J_{\text{P,C}} = 25\text{ Hz}, 3\text{ C}, \text{C}_{\text{benz}})$, $127.3(\text{d}, J_{\text{P,C}} = 2.0\text{ Hz}, 6\text{ C}, \text{C}_{\text{aryl}})$, $129.3(\text{d}, J_{\text{P,C}} = 2.1\text{ Hz}, 6\text{ C}, \text{C}_{\text{aryl}})$, $129.5(\text{s}, 6\text{ C}, \text{C}_{\text{aryl}})$, $130.3(\text{d}, ^4J_{\text{P,C}} = 6.4\text{ Hz}, 6\text{ C}, \text{C}_{\text{olef}})$, $131.7(\text{d}, J_{\text{P,C}} = 2.2\text{ Hz}, 6\text{ C}, \text{C}_{\text{aryl}})$, $134.5(\text{s}, 6\text{ C}, \text{C}_{\text{aryl,quat}})$, $135.1(\text{d}, J_{\text{P,C}} = 4.5\text{ Hz}, 6\text{ C}, \text{C}_{\text{aryl,quat}})$ ppm. $^{19}\text{F}\{^1\text{H}\}$ NMR (188.3 MHz, CD_3CN , 25°C): $\delta = -72.8(\text{d}, ^1J_{\text{P,F}} = 706\text{ Hz}, \text{PF}_6)$ ppm. $^{31}\text{P}\{^1\text{H}\}$ NMR (121.5 MHz, CD_3CN , 25°C): $\delta = 0.7(\text{s}, \text{trop}_3\text{P})$, $-144.5(\text{hept}, ^1J_{\text{P,F}} = 706\text{ Hz}, \text{PF}_6)$ ppm.

Preparation of (Chloro)[tris(5*H*-dibenzo[*a,d*]cyclohepten-5-yl)phosphane]rhodium(I) (6): In a Schlenk flask [Rh₂(μ-Cl)₂(COD)₂] (201 mg, 0.41 mmol) and trop₃P **1** (493 mg, 0.82 mmol) were suspended in THF (12 mL). This orange suspension was stirred at 60°C . Upon heating, all solids dissolved. After 30 h of stirring at 60°C , a pale yellow precipitate had formed and the ^{31}P NMR spectrum showed almost complete conversion. The mixture was left at -20°C overnight in order to complete crystallization. The precipitate was collected by filtration, washed with THF (5 mL), and dried in high vacuum. The product was a light yellow powder. Yield: 424 mg (70%). M.p. 320°C (starting decomposition). C₄₅H₃₃ClRh (743.08): calcd. C 72.74, H 4.48, P 4.17; found C 72.64, H 4.74. IR (ATR): $\tilde{\nu} = 3017(\text{w}, \nu_{\text{CH}})$, $1937(\text{w})$, $1599(\text{w})$, $1574(\text{w})$, $1483(\text{m})$, $1451(\text{m})$, $1417(\text{m})$, $1325(\text{w})$, $1286(\text{m})$, $743(\text{s})$, $731(\text{s})$, $643(\text{m})\text{ cm}^{-1}$. MS (EI): *m/z* 742 (M⁺), 191 (C₁₅H₁₁⁺). ^1H NMR (300 MHz, CD_2Cl_2 , 25°C): $\delta = 3.97(\text{d}, ^2J_{\text{P,H}} = 13\text{ Hz}, 3\text{ H}, \text{H}_{\text{benz}})$, $5.93(\text{s}, 6\text{ H}, \text{H}_{\text{olef}})$, $6.50(\text{d}, ^3J_{\text{H,H}} = 7.2\text{ Hz}, 6\text{ H}, \text{H}_{\text{aryl}})$, $6.77(\text{dd}, ^3J_{\text{H,H}} = 7.2\text{ Hz}, 7.2\text{ Hz}; 6\text{ H}, \text{H}_{\text{aryl}})$, $6.86(\text{dd}, ^3J_{\text{H,H}} = 7.2\text{ Hz}, 7.2\text{ Hz}; 6\text{ H}, \text{H}_{\text{aryl}})$, $7.02(\text{d}, ^3J_{\text{H,H}} = 7.2\text{ Hz}, 6\text{ H}, \text{H}_{\text{aryl}})$ ppm. $^{13}\text{C}\{^1\text{H}\}$ NMR (75.5 MHz, CD_2Cl_2 , 25°C): $\delta = 48.4(\text{d}, ^1J_{\text{P,C}} = 21.7\text{ Hz}, 3\text{ C}, \text{C}_{\text{benz}})$, $79.4(\text{d}, ^2J_{\text{P,C}} = 6.3\text{ Hz}, 6\text{ C}, \text{C}_{\text{olef}})$, $126.7(\text{s}, 6\text{ C}, \text{C}_{\text{aryl}})$, $127.1(\text{d}, J_{\text{P,C}} = 7.2\text{ Hz}, 6\text{ C}, \text{C}_{\text{aryl}})$, $127.5(\text{s}, 6\text{ C}, \text{C}_{\text{aryl}})$, $130.5(\text{s}, 6\text{ C}, \text{C}_{\text{aryl}})$, $133.7(\text{d}, J_{\text{P,C}} = 5.1\text{ Hz}, 6\text{ C}, \text{C}_{\text{aryl}})$, $135.6(\text{s}, 6\text{ C}, \text{C}_{\text{aryl}})$ ppm. $^{31}\text{P}\{^1\text{H}\}$ NMR (121.5 MHz, CD_2Cl_2 , 25°C): $\delta = 191.7(\text{d}, ^1J_{\text{Rh,P}} = 147.5\text{ Hz})$ ppm.

Preparation of (Chloro)[tris(5*H*-dibenzo[*a,d*]cyclohepten-5-yl)phosphane]iridium(I) (7): Because [Ir₂(μ-Cl)₂(coe)₄] is very air- and moisture-sensitive, the reaction was carried out under strictly inert conditions. In a Schlenk flask [Ir₂(μ-Cl)₂(coe)₄] (232 mg, 0.26 mmol) and **1** (314 mg, 0.52 mmol) were suspended in THF (18 mL). This orange suspension was stirred at 60°C . Upon heating, all the solids dissolved and the color darkened. After 70 h of stirring at 60°C the solution was dark brown and the ^{31}P NMR spectrum showed about 70% conversion to the product. The reaction mixture was filtered over Celite and the filtrate was concentrated. Leaving the sample at -20°C overnight allowed to crystallize the product in form of fine white needles. These were collected by filtration. To remove residual iridium metal, the product was dissolved in CH_2Cl_2 and filtered over a short silica gel column

($R_f = 0.3$). The product was precipitated with *n*-hexane and dried in high vacuum to give a white microcrystalline powder. Yield: 115 mg (53%). M.p. 340 °C (starting slight decomposition). $C_{45}H_{33}ClIrP$ (832.39): calcd. C 64.93, H 4.00, P 3.72; found C 64.72, H 4.03. IR (ATR): $\tilde{\nu} = 3014$ (w, ν_{CH}), 1600 (w), 1575 (w), 1483 (m), 1403 (w), 1286 (m), 746 (s), 732 (s), 644 (m) cm^{-1} . MS (EI): m/z 832 (M^+), 191 ($C_{15}H_{11}^+$). 1H NMR (300 MHz, CD_2Cl_2 , 25 °C): $\delta = 4.15$ (d, $^2J_{PH} = 13$ Hz, 3 H, H_{benz}), 5.40 (s, 6 H, H_{olef}), 6.46 (d, $^3J_{H,H} = 6.9$ Hz, 6 H, H_{aryl}), 6.70–6.84 (m, 12 H, H_{aryl}), 7.02 (d, $^3J_{H,H} = 6.9$ Hz, 6 H, H_{aryl}). $^{13}C\{^1H\}$ NMR (75.5 MHz, CD_2Cl_2 , 25 °C): $\delta = 44.8$ (d, $^1J_{PC} = 21.7$ Hz, 3 C, C_{benz}), 65.6 (s, 6 C, C_{olef}), 126.4 (s, 6 C, C_{aryl}), 127.6 (d, $J_{PC} = 7.5$ Hz, 6 C, C_{aryl}), 127.8 (d, $J_{PC} = 1.2$ Hz, 6 C, C_{aryl}), 131.7 (d, $J_{PC} = 1.6$ Hz, 6 C, C_{aryl}), 133.4 (d, $J_{PC} = 5.1$ Hz, 6 C, C_{aryl}), 135.7 (s, 6 C, C_{aryl}) ppm. $^{31}P\{^1H\}$ NMR (121.5 MHz, CD_2Cl_2 , 25 °C): $\delta = 134.1$ (s) ppm.

Preparation of (Aqua)[tris(5*H*-dibenzo[*a,d*]cyclohepten-5-yl)phosphane]palladium(II) Trifluoromethanesulfonate (9): In a Schlenk flask, $[PdCl_2(MeCN)_2]$ (166 mg, 0.43 mmol) and **1** (262 mg, 0.43 mmol) were suspended in acetonitrile (12 mL). This orange suspension was stirred at 60 °C. Upon heating, the suspension became red. After 24 h of stirring at 60 °C a dark red precipitate had formed and the ^{31}P NMR spectrum showed complete conversion. The mixture was left at –20 °C overnight in order to complete crystallization. The precipitate was collected by filtration and dried in high vacuum. The filtrate was evaporated to dryness and the residue dissolved in THF. A further crop of product was precipitated with *n*-hexane, collected by filtration, and subsequently dried in high vacuum for 24 h. ^{31}P NMR spectroscopy showed that this material consisted in majority of $[PdCl(trop_3P)]Cl$ [$\delta(^{31}P) = 263.8$ ppm] and some $[Pd(trop_3P)(MeCN)]Cl_2$ [$\delta(^{31}P) = 256.1$ ppm]. Subsequently, this product mixture (134 mg, 0.17 mmol) was dissolved in CH_2Cl_2 (15 mL) and $AgOTf$ (133 mg, 0.52 mmol) was added. The resulting suspension was stirred for 16 h. The color changed from dark red to dark ruby red. The suspension was filtered through Celite, concentrated, and the product was precipi-

tated with *n*-hexane. After washing with pentane, the dark ruby powder was dried in high vacuum. Yield: 162 mg (92%). M.p. 166–171 °C (decomposition). $C_{47}H_{35}F_6O_7PPdS_2$ (1027.29): calcd. C 54.95, H 3.43, P 3.02; found C 54.71, H 3.65. IR (ATR): $\tilde{\nu} = 3048$ (w, ν_{CH}), 1599 (w), 1507 (w), 1457 (m), 1431 (w), 1221 (s), 1159 (s), 1025 (s) 747 (s), 632 (s) cm^{-1} . UV (CH_2Cl_2): $\lambda_{max} = 497$ nm. 1H NMR (300 MHz, CD_2Cl_2 , 25 °C): $\delta = 5.79$ (d, $^2J_{PH} = 11$ Hz, 3 H, H_{benz}), 6.96–7.03 (m, 6 H, H_{aryl}), 7.05–7.13 (m, 12 H, H_{aryl}), 7.16–7.22 (m, 6 H, H_{aryl}), 7.40 (s, 6 H, H_{olef}) ppm. $^{13}C\{^1H\}$ NMR (75.5 MHz, CD_2Cl_2 , 25 °C): $\delta = 51.9$ (d, $^1J_{PC} = 16.0$ Hz, 3 C, C_{benz}), 109.6 (s, 6 C, C_{olef}), 128.5 (d, $J_{PC} = 1.4$ Hz, 6 C, C_{aryl}), 128.7 (d, $J_{PC} = 8.6$ Hz, 6 C, C_{aryl}), 129.4 (d, $J_{PC} = 5.1$ Hz, 6 C, C_{aryl}), 129.6 (d, $J_{PC} = 1.5$ Hz, 6 C, C_{aryl}), 131.3 (s, 6 C, C_{aryl}), 135.6 (d, $J_{PC} = 1.1$ Hz, 6 C, C_{aryl}) ppm. ^{19}F NMR (188.3 MHz, CD_2Cl_2 , 25 °C): $\delta = -78.1$ (br. s, 3 F), –77.9 (s, 3 F) ppm. $^{31}P\{^1H\}$ NMR (121.5 MHz, CD_2Cl_2 , 25 °C): $\delta = 270.6$ (s) ppm.

X-ray Crystallography: Crystals of **1** were grown from a THF solution that was layered with hexane. Crystals of **2** were obtained by slow cooling of a saturated toluene solution. Crystals of **3** grew from a reaction mixture of **4a** and nBu_4NCl in acetonitrile. Crystals of **5** were obtained by layering an acetonitrile solution of the compound with toluene. Crystals of **6** and **9** were grown by slow evaporation of THF and CH_2Cl_2 solutions, respectively. Data collection for the X-ray structure determinations were performed on Bruker SMART 1 K and SMART APEX platforms with graphite-monochromated Mo- K_α radiation ($\lambda = 0.71073$ Å). The reflex intensities were measured by CCD area detectors. The collected frames were processed with the proprietary software SAINT^[55] and an absorption correction was applied (SADABS^[56]). Solution and refinement of the structures was performed with SHELXS-97^[57] and SHELXL-97^[58] respectively. All non-hydrogen atoms were refined with anisotropic displacement parameters. Hydrogen atoms were placed in their idealized positions and allowed to ride on the respective carbon atoms. Associated crystallographic data and other experimental details are summarized in Table 4.

Table 4. Crystal data and refinement for compounds **1**, **2**, **3**, **5**, **6** and **9**.

	1	2 × ca. 0.5 $C_6H_5CH_3$	2 3 · $3CH_3CN$	5	6 ·2THF	2 9 · $3CH_2Cl_2$
Empirical formula	$C_{45}H_{33}P$	$C_{48.13}H_{33}PS$	$C_{96}H_{75}Ag_2Cl_2N_3P_2$	$C_{47}H_{36}AuF_6NP_2$	$C_{53}H_{49}ClO_2PRh$	$C_{97}H_{76}Cl_6F_{12}O_{14}P_2Pd_2S_4$
Formula mass	604.68	674.34	1619.17	987.67	887.25	2309.26
Crystal system	cubic	trigonal	monoclinic	orthorhombic	monoclinic	triclinic
Space group	$P\bar{4}3n$	$P\bar{3}$	$P2_1/c$	$Pbca$	$P2_1/n$	$P\bar{1}$
<i>a</i> [Å]	18.8014(6)	12.9046(3)	20.08(2)	16.8961(9)	11.9029(6)	15.4752(13)
<i>b</i> [Å]	18.8014(6)	12.9046(3)	12.045(14)	20.4423(11)	23.5360(12)	16.7033(14)
<i>c</i> [Å]	18.8014(6)	11.9912(4)	32.24(4)	23.0917(13)	15.8534(8)	21.8310(18)
α [°]	90	90	90	90	90	71.5240(10)
β [°]	90	90	106.32(2)	90	111.7970(10)	70.0620(10)
γ [°]	90	120	90	90	90	65.0040(10)
<i>V</i> [Å ³]	6646.2(4)	1729.35(8)	7485(15)	7975.8(8)	4123.7(4)	4708.0(7)
<i>Z</i>	8	2	4	8	4	2
<i>F</i> (000)	2544	706	3320	3904	1840	2332
Crystal size [mm]	$0.58 \times 0.45 \times 0.40$	$0.30 \times 0.28 \times 0.23$	$0.56 \times 0.29 \times 0.25$	$0.61 \times 0.52 \times 0.50$	$0.30 \times 0.28 \times 0.03$	$0.38 \times 0.33 \times 0.12$
$\rho_{calcd.}$ [g cm ^{−3}]	1.209	1.295	1.437	1.645	1.429	1.629
μ [cm ^{−1}]	0.114	0.175	0.690	3.833	0.561	0.763
<i>T</i> [K]	298	200	298	298	200	200
Rflns. collected	40979	15090	51917	69728	29373	23022
Unique rflns.	2283	2693	13039	8160	7028	16360
Flack parameter	0.10(19)	—	—	—	—	—
GOF on <i>F</i> ²	1.234	1.048	1.045	1.023	1.101	1.018
<i>R</i> ₁ , <i>wR</i> ₂	0.0545, 0.1577	0.0414, 0.1066	0.0315, 0.0795	0.0321, 0.0799	0.0374, 0.0863	0.0561, 0.1429
[<i>I</i> > 2σ(<i>I</i>)]						
<i>R</i> ₁ , <i>wR</i> ₂ (all data)	0.0579, 0.1626	0.0499, 0.1126	0.0504, 0.0909	0.0469, 0.0890	0.0466, 0.0902	0.0958, 0.1675

CCDC-622887 (for 1), -622888 (for 2), -622883 (for 3), -622884 (for 5), -622886 (for 6) and -622885 (for 9) contain the supplementary crystallographic data for this paper. These data can be obtained free of charge from The Cambridge Crystallographic Data Centre via www.ccdc.cam.ac.uk/data_request/cif.

Acknowledgments

The financial support of the ETHZ (Eidgenössische Technische Hochschule Zürich) and the SNF (Schweizerischer Nationalfonds) is gratefully acknowledged.

- [1] a) W. C. Zeise, *Ann. Phys. Chem.* **1831**, 21, 497–541; b) A. Cahours, A. W. Hofmann, *Ann. Chem. Pharm.* **1857**, 104, 1–39.
- [2] a) M. A. Bennett, R. S. Nyholm, J. Lewis, H. W. Kouwenhoven, *J. Chem. Soc.* **1964**, 4570–4577; b) L. V. Interrante, M. A. Bennett, R. S. Nyholm, *Inorg. Chem.* **1966**, 5, 2212–2217.
- [3] a) P. W. Clark, J. L. S. Curtis, P. E. Garrou, G. E. Hartwell, *Can. J. Chem.* **1974**, 52, 1714–1720; b) I. H. Wang, P. H. Wermer, C. B. Dobson, G. R. Dobson, *Inorg. Chim. Acta* **1991**, 183, 31–38.
- [4] P. E. Garrou, G. E. Hartwell, *J. Organomet. Chem.* **1973**, 55, 331–341.
- [5] a) P. H. Wermer, C. B. Dobson, G. R. Dobson, *J. Organomet. Chem.* **1986**, 311, C47–C50; b) S. L. Zhang, I. H. Wang, P. H. Wermer, C. B. Dobson, G. R. Dobson, *Inorg. Chem.* **1992**, 31, 3482–3488; c) H. H. Awad, G. R. Dobson, R. Vaneldik, *J. Chem. Soc., Chem. Commun.* **1987**, 1839–1841.
- [6] a) R. N. Haszeldine, R. J. Lunt, R. V. Parish, *J. Chem. Soc. A* **1971**, 3705–3711; b) P. E. Garrou, G. E. Hartwell, *J. Organomet. Chem.* **1974**, 71, 443–452.
- [7] a) M. B. Hursthouse, K. M. A. Malik, F. A. Hart, D. W. Owen, *Polyhedron* **1996**, 15, 23–26; b) W. Hewertson, I. C. Taylor, *J. Chem. Soc. D* **1970**, 428–429; c) S. Tsutsuminai, N. Komine, M. Hirano, S. Komiya, *Organometallics* **2004**, 23, 44–53.
- [8] a) G. E. Hartwell, P. W. Clark, *J. Chem. Soc. D* **1970**, 1115; b) P. W. Clark, G. E. Hartwell, *Inorg. Chem.* **1970**, 9, 1948–1951; c) P. W. Clark, G. E. Hartwell, *J. Organomet. Chem.* **1975**, 97, 117–129.
- [9] a) M. A. Bennett, R. S. Nyholm, J. D. Saxby, *J. Organomet. Chem.* **1967**, 10, 301–306; b) D. I. Hall, R. S. Nyholm, *J. Chem. Soc. A* **1971**, 1491–1493.
- [10] L. V. Interrante, G. V. Nelson, *J. Organomet. Chem.* **1970**, 25, 153–160.
- [11] a) M. A. Bennett, L. V. Interrante, R. S. Nyholm, *Z. Naturforsch., B: Chem. Sci.* **1965**, 20, 633–634; b) H. Luth, M. R. Truter, A. Robson, *J. Chem. Soc. A* **1969**, 28–41; c) I. H. Wang, G. R. Dobson, *J. Organomet. Chem.* **1988**, 356, 77–84.
- [12] L. V. Interrante, G. V. Nelson, *Inorg. Chem.* **1968**, 7, 2059–2063.
- [13] M. A. Bennett, G. B. Robertson, I. B. Tomkins, P. O. Whimp, *J. Chem. Soc. D* **1971**, 341–342.
- [14] a) M. A. Bennett, E. J. Hann, *J. Organomet. Chem.* **1971**, 29, C15–C16; b) P. R. Brookes, *J. Organomet. Chem.* **1972**, 42, 459–469; c) P. R. Brookes, *J. Organomet. Chem.* **1972**, 43, 415–423; d) D. I. Hall, R. Nyholm, *J. Chem. Soc., Dalton Trans.* **1972**, 804–808.
- [15] M. A. Bennett, W. R. Kneen, R. S. Nyholm, *Inorg. Chem.* **1968**, 7, 556–560.
- [16] a) M. A. Bennett, R. Bramley, I. B. Tomkins, *J. Chem. Soc., Dalton Trans.* **1973**, 166–168; b) M. A. Bennett, H. K. Chee, J. C. Jeffery, G. B. Robertson, *Inorg. Chem.* **1979**, 18, 1071–1076; c) M. A. Bennett, W. R. Kneen, R. S. Nyholm, *J. Organomet. Chem.* **1971**, 26, 293–303.
- [17] M. A. Bennett, W. R. Kneen, R. S. Nyholm, *Inorg. Chem.* **1968**, 7, 552–556.
- [18] a) E. Lindner, H. Rauleder, C. Scheytt, H. A. Mayer, W. Hiller, R. Fawzi, P. Wegner, *Z. Naturforsch., B: Chem. Sci.* **1984**, 39, 632–642; b) E. Lindner, C. Scheytt, *Z. Naturforsch., B: Chem. Sci.* **1986**, 41, 10–17; c) E. Lindner, C. Scheytt, P. Wegner, *J. Organomet. Chem.* **1986**, 308, 311–323.
- [19] a) A. F. Borowski, A. Iraqi, D. C. Cupertino, D. J. Irvine, D. J. Cole-Hamilton, M. H. Harmon, M. B. Hursthouse, *J. Chem. Soc., Dalton Trans.* **1990**, 29–34; b) D. J. Irvine, C. Glidewell, D. J. Cole-Hamilton, J. C. Barnes, A. Howie, *J. Chem. Soc., Dalton Trans.* **1991**, 1765–1772; c) D. C. Cupertino, M. M. Harding, D. J. Cole-Hamilton, *J. Organomet. Chem.* **1985**, 294, C29–C32; d) D. C. Cupertino, D. J. Cole-Hamilton, *J. Chem. Soc., Dalton Trans.* **1987**, 443–449.
- [20] D. J. Irvine, S. A. Preston, D. J. Cole-Hamilton, J. C. Barnes, *J. Chem. Soc., Dalton Trans.* **1991**, 2413–2418.
- [21] a) D. J. Irvine, A. F. Borowski, D. J. Cole-Hamilton, *J. Chem. Soc., Dalton Trans.* **1990**, 3549–3550; b) D. J. Irvine, D. J. Cole-Hamilton, J. Barnes, P. K. Hodgson, *Polyhedron* **1989**, 8, 1575–1577.
- [22] a) S. A. Preston, D. C. Cupertino, P. Palma-Ramirez, D. J. Cole-Hamilton, *J. Chem. Soc., Chem. Commun.* **1986**, 977–978; b) A. Iraqi, N. R. Fairfax, S. A. Preston, D. C. Cupertino, D. J. Irvine, D. J. Cole-Hamilton, *J. Chem. Soc., Dalton Trans.* **1991**, 1929–1935.
- [23] a) A. M. Z. Slawin, H. L. Milton, J. Wheatley, J. D. Woollins, *Polyhedron* **2004**, 23, 3125–3132; b) A. M. Z. Slawin, J. Wheatley, J. D. Woollins, *Eur. J. Inorg. Chem.* **2005**, 713–720.
- [24] a) P. W. Clark, G. E. Hartwell, *J. Organomet. Chem.* **1975**, 102, 387–396; b) P. W. Clark, G. E. Hartwell, *J. Organomet. Chem.* **1975**, 96, 451–459; c) M. A. Bennett, E. J. Hann, R. N. Johnson, *J. Organomet. Chem.* **1977**, 124, 189–211; d) P. E. Garrou, J. L. S. Curtis, G. E. Hartwell, *Inorg. Chem.* **1976**, 15, 3094–3097; e) R. R. Ryan, R. Schaeffer, P. Clark, G. Hartwell, *Inorg. Chem.* **1975**, 14, 3039–3042.
- [25] a) M. O. Visscher, J. C. Huffman, W. E. Streib, *Inorg. Chem.* **1974**, 13, 792–797; b) D. I. Hall, R. S. Nyholm, *J. Chem. Soc. D* **1970**, 488–489; c) C. Nave, M. R. Truter, *J. Chem. Soc. D* **1971**, 1253–1254; d) C. Nave, M. R. Truter, *J. Chem. Soc., Dalton Trans.* **1973**, 2202–2204; e) P. W. Clark, A. J. Jones, *J. Organomet. Chem.* **1976**, 122, C41–C48.
- [26] M. Herberhold, K. Bauer, W. Milius, *Z. Anorg. Allg. Chem.* **1994**, 620, 2108–2113.
- [27] M. Herberhold, T. Schmalz, W. Milius, B. Wrackmeyer, *Inorg. Chim. Acta* **2002**, 334, 10–16.
- [28] a) M. Herberhold, K. Bauer, W. Milius, *J. Organomet. Chem.* **1997**, 546, 267–275; b) M. Herberhold, K. Bauer, W. Milius, *Z. Naturforsch. B: Chem. Sci.* **1999**, 54, 63–72.
- [29] a) M. Herberhold, A. Pfeifer, W. Milius, *Z. Anorg. Allg. Chem.* **2002**, 628, 2919–2929; b) M. Herberhold, W. Milius, A. Pfeifer, *Z. Naturforsch. B: Chem. Sci.* **2003**, 58, 1–10; c) M. Herberhold, W. Milius, A. Pfeifer, *Z. Naturforsch. B: Chem. Sci.* **2003**, 58, 11–15.
- [30] M. Herberhold, K. Bauer, W. Milius, *J. Organomet. Chem.* **1998**, 563, 227–233.
- [31] a) M. Herberhold, W. Milius, S. Eibl, *Z. Anorg. Allg. Chem.* **1999**, 625, 341–346; b) M. Herberhold, S. Eibl, W. Milius, B. Wrackmeyer, *Z. Anorg. Allg. Chem.* **2000**, 626, 552–555; c) M. Herberhold, S. Eibl, W. Milius, *J. Organomet. Chem.* **2001**, 621, 166–172.
- [32] a) M. Herberhold, T. Schmalz, W. Milius, B. Wrackmeyer, *Z. Anorg. Allg. Chem.* **2002**, 628, 437–445; b) M. Herberhold, T. Schmalz, W. Milius, B. Wrackmeyer, *J. Organomet. Chem.* **2002**, 641, 173–184; c) M. Herberhold, T. Schmalz, W. Milius, B. Wrackmeyer, *Z. Naturforsch. B: Chem. Sci.* **2002**, 57, 53–60; d) M. Herberhold, T. Schmalz, W. Milius, B. Wrackmeyer, *Z. Anorg. Allg. Chem.* **2002**, 628, 979–986; e) M. Herberhold, T. Schmalz, W. Milius, B. Wrackmeyer, *Inorg. Chim. Acta* **2003**, 352, 51–60.
- [33] M. Herberhold, T. Schmalz, W. Milius, B. Wrackmeyer, *Z. Naturforsch. B: Chem. Sci.* **2002**, 57, 255–258.

- [34] a) M. Herberhold, N. Akkus, W. Milius, *Z. Naturforsch. B: Chem. Sci.* **2003**, 58, 528–532; b) M. Herberhold, W. Milius, N. Akkus, *Z. Anorg. Allg. Chem.* **2006**, 632, 97–100.
- [35] M. Herberhold, N. Akkus, W. Milius, *Z. Anorg. Allg. Chem.* **2003**, 629, 2458–2464.
- [36] J. Thomaier, Diss. Albert-Ludwigs-Universität (79104 Freiburg, Germany), **1996**.
- [37] a) S. Deblon, Diss. ETH Nr. 13920 (Zürich), **2000**; b) P. Maire, Diss. ETH Nr. 14396 (Zürich), **2001**; c) C. Böhrer, Diss. ETH Nr. 14420 (Zürich), **2002**; d) C. Laporte, C. Böhrer, H. Schönberg, H. Grützmacher, *J. Organomet. Chem.* **2002**, 641, 227–234; e) C. Laporte, F. Breher, J. Geier, J. Harmer, A. Schweiger, H. Grützmacher, *Angew. Chem.* **2004**, 116, 2621–2624; *Angew. Chem. Int. Ed.* **2004**, 43, 2567–2570; f) C. Laporte, T. Büttner, H. Rüegger, J. Geier, H. Schönberg, H. Grützmacher, *Inorg. Chim. Acta* **2004**, 357, 1931–1947; g) C. Laporte, Diss. ETH Nr. 15137 (Zürich), **2003**; h) P. Maire, S. Deblon, F. Breher, J. Geier, C. Böhrer, H. Rüegger, H. Schönberg, H. Grützmacher, *Chem. Eur. J.* **2004**, 10, 4198–4205.
- [38] a) H. Schönberg, S. Boulmaaz, M. Wörle, L. Liesum, A. Schweiger, H. Grützmacher, *Angew. Chem.* **1998**, 110, 1492–1494; *Angew. Chem. Int. Ed.* **1998**, 37, 1423–1426; b) S. Boulmaaz, M. Mlakar, S. Loss, H. Schönberg, S. Deblon, M. Wörle, R. Nesper, H. Grützmacher, *Chem. Commun.* **1998**, 2623–2624.
- [39] J. Thomaier, S. Boulmaaz, H. Schönberg, H. Rüegger, A. Currao, H. Grützmacher, H. Hillebrecht, H. Pritzkow, *New J. Chem.* **1998**, 22, 947–958.
- [40] a) S. Deblon, L. Liesum, J. Harmer, H. Schönberg, A. Schweiger, H. Grützmacher, *Chem. Eur. J.* **2002**, 8, 601–611; b) M. Mlakar, S. Boulmaaz, H. Schönberg, H. Grützmacher, *Electroanalysis* **2003**, 15, 1043–1053; c) S. Deblon, H. Rüegger, H. Schönberg, S. Loss, V. Gramlich, H. Grützmacher, *New J. Chem.* **2001**, 25, 83–92.
- [41] R. Kissner, P. Latal, G. Geier, *J. Chem. Soc., Chem. Commun.* **1993**, 136–137.
- [42] a) R. Kissner, *J. Electroanal. Chem.* **1995**, 385, 71–75; b) R. Kissner, G. Welter, G. Geier, *J. Chem. Soc., Dalton Trans.* **1997**, 1773–1777.
- [43] A. G. Orpen, L. Brammer, F. H. Allen, O. Kennard, D. G. Watson, R. Taylor, *J. Chem. Soc., Dalton Trans.* **1989**, S1–S83.
- [44] A somewhat larger cone angle (265°) was reported for the triarylphosphane(2,6-*i*Pr-C₆H₃)₃P: R. T. Boeré, Y. K. Zhang, *J. Organomet. Chem.* **2005**, 690, 2651–2657.
- [45] M. Herberhold, K. Bauer, W. Milius, *J. Organomet. Chem.* **1995**, 502, C1–C4.
- [46] a) E. Lindner, R. Fawzi, H. A. Mayer, K. Eichele, K. Pohmer, *Inorg. Chem.* **1991**, 30, 1102–1107; b) M. D. Lumsden, K. Eichele, R. E. Wasylishen, T. S. Cameron, J. F. Britten, *J. Am. Chem. Soc.* **1994**, 116, 11129–11136.
- [47] For a recent second example of a [Au(PR₃)(MeCN)]⁺ complex, see: Q. S. Li, C. Q. Wan, R. Y. Zou, F. B. Xu, H. B. Song, X. J. Wan, Z. Z. Zhang, *Inorg. Chem.* **2006**, 45, 1888–1890.
- [48] I. Krossing, A. Reisinger, *Angew. Chem.* **2003**, 115, 5903–5906; *Angew. Chem. Int. Ed.* **2003**, 42, 5725–5728.
- [49] D. Ostendorf, C. Landis, H. Grützmacher, *Angew. Chem.* **2006**, 118, 5293–5297; *Angew. Chem. Int. Ed.* **2006**, 45, 5169–5173.
- [50] G. Berti, *J. Org. Chem.* **1957**, 22, 230–230.
- [51] H. H. Karsch, *Phosphorus, Arsenic, Antimony and Bismuth*, vol. 3, Thieme, Stuttgart, **1996**.
- [52] J. L. Herdè, C. V. Senoff, *Inorg. Nucl. Chem. Lett.* **1971**, 7, 1029–1031.
- [53] R. K. Harris, E. D. Becker, S. M. C. De Menezes, R. Goodfellow, P. Granger, *Pure Appl. Chem.* **2001**, 73, 1795–1818.
- [54] M. Bak, J. T. Rasmussen, N. C. Nielsen, *J. Magn. Reson.* **2000**, 147, 296–330.
- [55] *SAINT, Reference manual*, Siemens Energy and Automation, Madison, WI, **1994–1996**.
- [56] G. M. Sheldrick, *SADABS, Empirical Absorption Correction Program*, University of Göttingen, Germany, **1997**.
- [57] G. M. Sheldrick, *SHELXS-97, Program for Crystal Structure Solution*, University of Göttingen, Germany, **1997**.
- [58] G. M. Sheldrick, *SHELXL-97, Program for Crystal Structure Refinement*, University of Göttingen, Germany, **1997**.

Received: October 25, 2006

Published Online: January 25, 2007